UNIVERSITAT DE BARCELONA

ADVANCED MATHEMATICS
MASTER'S FINAL PROJECT

Study of volume-preserving flows guided by the Michelson system

---

Author:
Ainoa Murillo López

Supervisor:
Arturo Vieiro Yanes

Facultat de Matemàtiques i Informàtica

September 7, 2020

Abstract

We consider three-dimensional volume preserving flows and we study aspects of its dynamics. We describe the geometry of flows having a volume-preserving symmetry. Perturbations of such flows are reduced to Poincaré (not necessarily canonical) area-preserving maps. We present a detailed study of the phase space of area-preserving maps through Birkhoff normal form. These results are illustrated for the Michelson system. Comments on the asymptotic behaviour of the splitting of the invariant manifolds of this system are given. Finally, we include a preliminar description of the dynamics of a discretization of the Michelson flow. It shows up a richer dynamics than the flow that we try to show through some numerical investigations.

Resum

Es consideren fluxos tridimensionals que preserven volum i estudiem aspectes de la seva dinàmica. Es descriu la geometria dels fluxos que admeten una simetria que preserva volum. Les pertorbacions d'aquests fluxos es redueixen a mapes de Poincaré que preserven una forma d'àrea no necessàriament canònica. Es presenta un estudi detallat de l'espai de fase de mapes que preserven l'àrea a través de la forma normal de Birkhoff. Aquests resultats es mostren pel sistema de Michelson i es comenta el comportament asimptòtic de l'escissió de les varietats invariants del sistema. Finalment, s'inclou una descripció preliminar de la dinàmica d'una discretització del flux de Michelson. Aquesta, mostra una dinàmica més rica que la del flux que intentem il·lustrar a través de diverses investigacions numèriques.

Acknowledgments

To my supervisor, Arturo Vieiro, for his absolute availability, patience and support. For the enthusiasm he passes on me and the encouragement in difficult moment. Thank you so much.
To my family, specially to my parents, for their unconditional support.

Contents

The aim of this work is to study the dynamics of three-dimensional volume-preserving flows. This flows are of interest in applications since they appear naturally from fluid convection problems. In 1966, Arnold observed that in a three-dimensional flow associated to a fluid convection problem, the Poincaré map was chaotic and that the topology of the orbits was not trivial. Later, Hénon did some numerical studies to confirm this behaviour, see [4] and [21].

In this work we will present some results that allow us to understand the topology of those orbits. Indeed, we will present most of the results through the study of the Michelson flow. We will see that the Michelson system can be seen as a perturbation of an integrable system showing up a Hill's spherical vortex. This spherical vortex is a rotational solution of the Euler equations [7] of an incompressible flow without viscosity.

The Michelson system is a paradigm of three dimensional flows of this type that it has been extensively studied in the literature. Due to the fact that it is related to steady state solutions of the Kuramoto-Shivashinsky equation it drew the attention of researches in physical and mathematical areas. Mathematically, it is an important model that appears at the unfolding of the Hopf-zero bifurcation, see [15], where dissipative versions of the model studied here appear for suitable parameters in the unfolding of such codimension two bifurcation. Even though the Michelson system is a simple quadratic three dimensional conservative flow, it shows up different phenomena, including homo/heteroclinic phenomena, which makes its dynamics very rich.

On the other hand, the dynamics of a time-periodic incompressible flow can be described by a three-dimensional volume-preserving map, so in the last Chapter of this work we will present some preliminary results and discuss the main difficulties that we found when studying the dynamics of a discretization of the Michelson flow.

Besides, the study of three-dimensional volume preserving flows with a recurrence in the phase space leads to the study of two-dimensional maps that preserve an area form. This reduction is achieved by choosing a suitable Poincaré section. Hence, we have also used different techniques to study the dynamics of area preserving maps. Since we do not have the map explicitly, we have also used numerical techniques to study the Poincaré map, as for example the jet transport method to get the Taylor expansion of this map, that we can use to reduce it to normal form. In the study of three dimensional flows and maps, we include computations of the invariant manidolds that lead us to use multiprecision arithmetics. Also several of the algorithms used require the implementation of an algebraic manipulator to deal with polynomials. We have used the internal routines of PARI/GP, [10], to simplify the implementations.

In Chapter 1 we will introduce three dimensional volume-preserving flows with volume-preserving symmetries, and we will see that under certain conditions, the system could have some Hamiltonian structure. Moreover, we will give a general overview on the Michelson system, and in particular, we will see that for small enough values of the parameter it can be seen as a perturbation of a system that possesses a rotational symmetry.

In order to study the dynamics of a three-dimensional conservative flow, the reduction to a Poincaré map will be considered in Chapter 2. We will prove that this Poincaré map is indeed an area preserving map. In general, this two-dimensional map does not preserve

the canonical area form. Nevertheless, as a consequence of Darboux's theorem, we know that there exists a change of coordinates that locally relates any two symplectic forms. We include the corresponding statement and the proof of the theorem. There are different ways to prove this theorem, here we will use the so-called Moser trick.
Moreover, in chapter 2, we also include a description of the main properties of the phase space of the Poincaré map through illustrations obtained for different values of the parameter for the Michelson system.

Chapter 3 is devoted to study the dynamics of area preserving maps around an elliptic fixed point using the Birkhoff normal form reduction. The Birkhoff normal form, in general, is not convergent, but we will see that truncated to a suitable order, allow us to obtain a detailed description of the phase space around the fixed point. In particular, we will prove that the truncated Birkhoff normal form can be written as a rotation composed with a near-the-identity map, that can be interpolated by a time-1 flow of a Hamiltonian. This expression of the BNF in terms of the Hamiltonian allow us to study the existence of periodic fixed points and the structure of resonant islands. In addition, we will discuss the persistence of invariant curves of the Poincaré map when perturbing the system, or equivalently, the persistence of invariant tori of the flow.

Moreover, for the Michelson flow, we will see that the two-dimensional invariant manifolds of the fixed points confine a family of invariant tori around an elliptic periodic orbit. The intersection of the invariant manifolds and the asymptotic behaviour of their splitting are described in Chapter 4.

Chapter 5 attempts to illustrate some aspects of the dynamics of the Michelson map, which is a volume-preserving map obtained as a discretization of the Michelson flow. In particular, we perform different computations of the invariant manifolds and compute some orbits of the continuum of heteroclinic orbits of the map. These orbits lie in the intersection of the two-dimensional invariant manifolds of the saddle-focus fixed points.

Also in Chapter 5 we will discuss the differences with the Michelson flow, and state several questions that remain open in this setting. Some extra general conclusions are given at the end of the work.

Chapter 1

Conservative 3D flows with volume-preserving symmetries

The aim of this chapter is to give a general overview of volume-preserving flows with symmetry. Moreover, we will also provide a general study of the Michelson system and will see that it can be seen as a perturbation of a volume-preserving system with symmetries.

1.1 Basic properties of the Michelson system

The Michelson system

$$\begin{cases} \dot{x} = y \\ \dot{y} = z \\ \dot{z} = \varepsilon(1 - x^2) - y \end{cases} \tag{1.1}$$

is a three dimensional system $\dot{x} = X_\varepsilon(x)$ of ordinary differential equations with a parameter $\varepsilon \geqslant 0$, that appears as the equation for travelling wave solutions of a non-linear partial differential equation called the Kuramoto-Sivashinsky equation, [30]

$$u_t + u_{xxxx} + u_{xx} + \frac{1}{2}u_x^2 = 0.$$

The Michelson flow is clearly volume-preserving since it is divergence free

$$divX_\varepsilon = trDX_\varepsilon = tr \begin{pmatrix} 0 & 1 & 0 \\ 0 & 0 & 1 \\ -\varepsilon 2x & -1 & 0 \end{pmatrix} = 0,$$

by Liouville's theorem, that we briefly recall here for three dimensional flows (it holds in $\mathbb{R}^n$ as well)[1].

[1]We will omit several proof of standards theorem that can be found in common references on ordinary differential equations or dynamical systems, see [6, 3, 32, 37].

Theorem 1.1 (Liouville). *Let $F : U \subset \mathbb{R}^3 \longrightarrow \mathbb{R}^3$ be a three dimensional vector field $\mathcal{C}^r, r \geqslant 1$ such that φ_t is the flow induced by $\dot{x} = F(x)$ and $\Omega(t)$ is the volume of the image, $\varphi_t(D)$ of any region D of its phase space. If $divX \equiv 0$, then φ_t preserves volume, i.e. $\Omega(t) = \Omega(0)$ for all t.*

The Michelson system has the property of being a reversible system. Concretely, is invariant under the involution $R(x, y, z) = (-x, y, -z)$ and the time reverse $t \longmapsto -t$. This can be easily checked since

$$R \circ X_\varepsilon(x) = (-y, z, -\varepsilon(1 - x^2) + y) = -X_\varepsilon \circ R(x).$$

This property of being reversible imposes some intrinsic symmetries in the set of solutions of the system that, in particular, can be exploited to simplify computations.

In order to study the dynamics of the system, we will start doing the analysis of the fixed points, local bifurcations and the invariant manifolds.

For $\varepsilon > 0$, the Michelson system has fixed points $x_+ = (1, 0, 0)$ and $x_- = R(x_+)$ since $X_\varepsilon(x_\pm) = 0$. To study the stability of these points with respect to the parameter ε, one consider the linearised system at $x_\pm$ and study the eigenvalues of

$$DX_\varepsilon(x_\pm) = \begin{pmatrix} 0 & 1 & 0 \\ 0 & 0 & 1 \\ -2\varepsilon x & -1 & 0 \end{pmatrix}.$$

Thus the eigenvalues are solutions of the equation $P(\lambda) = \lambda^3 + 2\varepsilon x + \lambda = 0$.

The characteristic polynomial P has a real root and, since the discriminant $\Delta = -4 - 27(2\varepsilon x)^2 = -4 - 108\varepsilon^2 x^2 < 0$ is negative, the other two roots are complex conjugated. Therefore the eigenvalues of $DX(x_\pm)$ are

$$\lambda_{x_\pm} \in \mathbb{R}, \qquad \mu^\pm_{x_\pm} = \frac{-\lambda_{x_\pm} \pm i\sqrt{3\lambda^2_{x_\pm} + 4}}{2} \in \mathbb{C}.$$

In this case both fixed points $x_\pm$ are hyperbolic and then Hartman-Grobman theorem, see for example [32, 37], guarantees that the dynamics of the linearized system is topologically conjugated to the local dynamics of the system around $x_\pm$.

Since $\lambda_{x_\pm}$ satisfies $\lambda^3 + \lambda = -2\varepsilon x$ and , $\mu^\pm_{x_\pm} = \frac{-\lambda_{x_\pm} \pm i\sqrt{3\lambda^2_{x_\pm}+4}}{2}$ we have

$$\begin{aligned} &\lambda_{x_+} < 0, Re(\mu^\pm_{x_+}) > 0, \qquad \text{for } x_+ = (1, 0, 0), \\ &\lambda_{x_-} > 0, Re(\mu^\pm_{x_-}) < 0, \qquad \text{for } x_- = (-1, 0, 0). \end{aligned}$$

Thus $x_\pm$ are saddle-focus fixed points and the stable manifold theorem, see for example [32], gives the existence of the corresponding stable and unstable invariant manifolds, denoted as W^s and W^u respectively. In this case the dimension of these manifolds are $\dim W^u(x_+) = \dim W^s(x_-) = 2$ and $\dim W^s(x_+) = \dim W^u(x_-) = 1$. These manifolds are smooth (analytic) and tangent at the hyperbolic point $x_\pm$ to the eigenspaces of dimension two, and one respectively, generated by eigenvectors of $DX_\varepsilon(x_\pm)$.

When $\varepsilon = 0$, the Michelson system has the origin as a fixed point having eigenvalues 0 and $\pm i$. Moreover Michelson proved in [30] the existence of a periodic orbit for $\varepsilon > 0$ sufficiently small, which tends to the origin when ε tends to zero. That is the Michelson system has a Hopf-zero bifurcation at the origin for $\varepsilon \geqslant 0$ sufficiently small.
See comments on the Hopf-zero bifurcation and its unfolding in section 4.2. An analytic proof of the existence of this bifurcation is given in [23].

For ε small enough, the two-dimensional invariant manifolds confine a Cantor family of invariant tori around an elliptic invariant circle. Since they almost coincide for small ε, the previous structure resembles a bubble of stability of the system (1.2). In section 4.2 we will describe the asymptotic behaviour of the splitting of theses manifolds as $\varepsilon \longrightarrow 0$. It behaves in an exponential small way in ε, as expected in the analytic category for conservative systems. This justifies the previous assertion that they bound a "bubble" of stability. The Michelson flow has heteroclinic orbits given by the intersection of the two-dimensional invariant manifolds as we will see in section 4.1.

In order to obtain a qualitative description of the phase space of the Michelson when ε tends to zero, we introduce variables $s = x + z$, $y = R\cos\theta$ and $z = R\sin\theta$,

$$\begin{aligned}
\dot{\theta} &= \frac{d}{dt}\arctan(z/y) = \frac{\dot{z}y - z\dot{y}}{y^2+z^2} = -1 + \frac{\varepsilon(1-x^2)R\cos\theta}{R^2} = -1 + \mathcal{O}\left(\frac{\varepsilon}{R}\right),\\
\dot{s} &= \dot{x} + \dot{z} = \varepsilon(1-(s-R\sin\theta)^2),\\
\dot{R} &= \frac{y\dot{y} + z\dot{z}}{R} = \varepsilon\sin\theta(1-(s-R\sin\theta)^2).
\end{aligned}$$

We observe that the angle θ is a fast angle. Performing one step of averaging over this fast angle, we obtain

$$\dot{\theta} = -1, \qquad \dot{s} = \varepsilon\left(1 - s^2 - \frac{R^2}{2}\right), \qquad \dot{R} = \varepsilon R s. \tag{1.2}$$

where we have used the fact that sin is an odd function and only those terms in $\sin(\theta)^2$ contribute to the averaged system (1.2) with a factor $1/2$. In the previous expression (1.2), the omitted terms add a relative error ε/R that will be ignored in the qualitative description below.
Due to the uncoupled structure of (1.2) we can study the evolution of the s, R coordinates independently. The corresponding two-dimensional system is Hamiltonian, with $H(s,R) = R^2(1 - s^2 - R^2/4)$ and with the symplectic 2-form $\varepsilon(dx \wedge dy)$. In Figure 1.1 we can see the main features of the reduced system, it has two fixed points of saddle type with one-dimensional heteroclinic connections.
The periodic orbits observed in the figure are two-dimensional invariant tori of the integrable system (1.2). This system has rotational symmetry, see related comments below. Since the Michelson system, for small ε, can be seen as a perturbation of (1.2), we expect the system to have bounded orbits. This is a consequence of perturbation results based on KAM theory 3.5. Hence when ε decreases, the measure of the set of orbits of (1.1) grows.

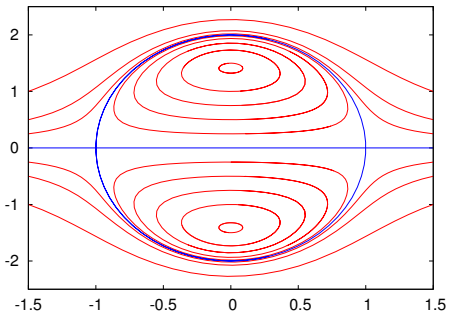

Figure 1.1: Phase space of the reduced two-dimensional system in variables s, R.

1.2 Geometric structure of three dimensional flows with symmetry

Three-dimensional flows are relevant in applications, for example, the study of chaotic advection leads naturally to a three-dimensional flow, see [4, 21]. Here, we want to investigate geometrical properties of such flows.

The odd dimension of the phase space imposes some restrictions of the structure. For example, the zero-energy level of a two degrees of freedom autonomous Hamiltonian defines a three dimensional flow on a suitable manifold. Nevertheless it is not true that any three dimensional flow is realised as a zero-energy level of a two-degree of freedom autonomous C^2 Hamiltonian, because the Hamiltonian structure implies preservation of area in pairs of symplectic conjugated components.

The fact that a general three dimensional flow does not posses a Hamiltonian structure, difficult the analytical study of transport properties. Fortunately, in several situations, the flow under considerations can be seen as a perturbation of a system having a volume preserving symmetry (see definition below). When the three dimensional flow possesses a volume preserving symmetry, then, in a suitable 3d manifold, one can introduce symplectic conjugated coordinates, so that the reduced flow becomes Hamiltonian. The level set of this Hamiltonian are surfaces through which one can attempt to study the flux of the system.

To state the result properly we introduce some general background in Lie group theory. Let us consider the system $\dot{x} = F(x,t)$ defined on an open domain $U \times I \subset \mathbb{R}^3 \times \mathbb{R}$.

Definition 1.2. Consider the family of maps

$$\begin{aligned} g : & U \times \mathbb{R} \times I \longrightarrow U \times \mathbb{R} \\ & (x,t;\lambda) \quad \longmapsto g(x,t;\lambda) \end{aligned}$$

which depend of the parameter $\lambda \in I$. We say that this family of maps forms a *one-parameter Lie group* G acting on $U \times \mathbb{R}$ if it satisfies the following properties:

1. For each $\lambda \in I$, g is one-to-one and onto $U \times \mathbb{R}$. The maps are infinitely differentiable with respect to $(x,t) \in U \times \mathbb{R}$ and analytic in $\lambda \in I$.

2. I forms a group with an analytic law of composition $\phi(\lambda, \delta) : I \times I \longrightarrow I$.

3. $(x, t) = g(x, t; e)$, where e is the identity element in the group (I, ϕ).

4. If $(x^1, t^1) = g(x^0, t^0; \lambda^0)$ and $(x^2, t^2) = g(x^1, t^1; \lambda^1)$, then $(x^2, t^2) = g(x^0, t^0; \phi(\lambda^0, \lambda^1))$.

Let $g_i, i = 1, \ldots 4$ be the components of G.

Definition 1.3. The *infinitesimal generator* of the action of G is the vector field w on $U \times I$ given by

$$w = \sum_{i=1}^{3} \xi_i(x, t) \frac{\partial}{\partial x_i} + \xi_4(x, t) \frac{\partial}{\partial t},$$

where $\xi_i(x, t) = \frac{\partial g_i}{\partial \lambda}(x, t, 0)$, for $i = 1, \ldots, 4$.

Definition 1.4. Let G be a one-parameter Lie group acting on $U \times I$. We say that $\dot{x} = F(x, t)$ admits a *one-parameter group of symmetries* G if and only if whenever $\varphi(t)$ is a solution then so is $g(\varphi(t), t, \lambda)$, where $g(x, t, \lambda)$ is any element of G.

Definition 1.5. A one parameter Lie group G is a *spatial symmetry group* if it acts only on the dependent variables and its infinitesimal generator is an autonomous vector field on $\mathbb{R}^3$, that is, $w \equiv \sum_{i=1}^{3} \xi_i(x, t) \frac{\partial}{\partial x_i}$.
A spatial symmetry group is volume preserving if its infinitesimal generator is a volume preserving vector field.

Let us show that the Michelson system (1.1), for ε small enough can be seen as a perturbation of the system (1.2), that possesses a rotational symmetry. We express the system (1.2) in cartesian coordinates $s, y = R\cos\theta, z = R\sin\theta$,

$$\begin{aligned} \dot{s} &= \varepsilon \left(1 - s^2 - \frac{y^2 + z^2}{2}\right), \\ \dot{y} &= \varepsilon s y - z, \\ \dot{z} &= \varepsilon s z + y. \end{aligned}$$

and let G be the spatial symmetry group that form the rotation matrices around the s axis, that is,

$$G := \{R^s_\lambda, \lambda \in \mathbb{R}\}, \qquad R^s_\lambda = \begin{pmatrix} 1 & 0 & 0 \\ 0 & \cos\lambda & -\sin\lambda \\ 0 & \sin\lambda & \cos\lambda \end{pmatrix}. \tag{1.3}$$

To prove that the system (1.2) admits G we have to see that given $\varphi(t) = (s(t), y(t), z(t))^T$ a solution then $\tilde{\varphi}(t) = (\tilde{s}(t), \tilde{y}(t), \tilde{z}(t))^T = R^s_\lambda (s(t), y(t), z(t))^T$ is also a solution for all $\lambda \in \mathbb{R}$,

$$\tilde{\varphi}(t) = (s(t), \cos\lambda y(t) - \sin\lambda z(t), \sin\lambda y(t) + \cos\lambda z(t))^T.$$

Note that $\tilde{y}^2+\tilde{z}^2 = \cos\lambda^2 y^2 + \sin\lambda^2 z^2 - 2\sin\lambda\cos\lambda yz + \sin\lambda^2 y^2 + \cos\lambda^2 z^2 + 2\sin\lambda\cos\lambda yz = (y^2+z^2)$. Hence

$$\begin{aligned}
\dot{\tilde{s}} &= \varepsilon\left(1-\tilde{s}^2-\frac{\tilde{y}^2+\tilde{z}^2}{2}\right),\\
\dot{\tilde{y}} &= \cos\lambda\dot{y}-\sin\lambda\dot{z} = \varepsilon\tilde{s}(\cos\lambda y-\sin\lambda z)-(\cos\lambda z-\sin\lambda y) = \varepsilon\tilde{s}\tilde{y}-\tilde{z},\\
\dot{\tilde{z}} &= \sin\lambda\dot{y}+\cos\lambda\dot{z} = \varepsilon\tilde{s}(\sin\lambda y-\cos\lambda z)+(\sin\lambda z-\cos\lambda y) = \varepsilon\tilde{s}\tilde{z}-\tilde{y}.
\end{aligned}$$

Therefore $\tilde{\varphi}(t) = R^s_\lambda\varphi(t)$ is a solution of the system.

One has $g(x,t;\lambda) = R^s_\lambda(x)$, hence the infinitesimal generator of G is the autonomous vector field

$$\begin{aligned}
w &= \sum_{i=1}^{3}\frac{\partial g_i}{\partial\lambda}(x,t,0)\frac{\partial}{\partial x_i} = \frac{\partial g_2}{\partial\lambda}(x,t,0)\frac{\partial}{\partial x_2}+\frac{\partial g_3}{\partial\lambda}(x,t,0)\frac{\partial}{\partial x_3}\\
&= -x_3\frac{\partial}{\partial x_2}+x_2\frac{\partial}{\partial x_3}.
\end{aligned}$$

Any three dimensional flow, not necessarily autonomous, that is invariant under the action of a volume-preserving symmetry group can be transformed to a form where two components have canonical form of a one degree of freedom Hamiltonian system, not necessarily autonomous, and the third component depends only on the first two variables. This is the content of the following theorem stated in [29].

Theorem 1.6. *Let*

$$\frac{dx_i}{dt} = f_i(x_1,x_2,x_3,t), \qquad i=1,\cdots,3,$$

be a volume-preserving system that it admits a one-parameter spatial volume-preserving symmetry group G. Then there exists a local volume preserving change of variables $x_i = \phi_i(z_1,z_2,z_3), i = 1,\cdots,3$, such that the system becomes

$$\begin{aligned}
\frac{dz_1}{dt} &= \frac{\partial H(z_1,z_2,t)}{\partial z_2},\\
\frac{dz_2}{dt} &= -\frac{\partial H(z_1,z_2,t)}{\partial z_1},\\
\frac{dz_3}{dt} &= k_3(z_1,z_2,t).
\end{aligned}$$

where z_1, z_2 are functionally independent invariants of G.
If the original system is autonomous, so it is the transformed system, and H is a first integral.

Sketch of the proof. The construction of the change of variables ϕ consists in different steps.

1. In [31], Olver proves that given a system $\dot{x} = F(x,t)$ that admits a one parameter group of symmetries G, and given a regular point $p = (x,t) \in U\times I$ of the vector field w, there exists a local change of coordinates

$$(y,s) = (\phi_{1,y}(x,t),\phi_{1,s}(x,t)),$$

that transform the system into

$$\frac{d}{ds}y_i = \tilde{F}_i(y_1, y_2, s), \qquad i = 1, \ldots, 3,$$

where y_1, y_2 and s are functionally independent invariants of G, and $L_w(y_3) = 1$. Here, $L_w(y_3)$ denotes the Lie derivative of y_3 with respect to the vector field w [2].

2. If G is a spatial symmetry group, one has that t is invariant by the action of G. One can take then $s = t$. Moreover, since w is autonomous, y_1, y_2 and y_3 are independent.

3. Next, the system

$$\frac{d}{dt}y_1 = \tilde{F}_1(y_1, y_2, t),$$
$$\frac{d}{dt}y_2 = \tilde{F}_2(y_1, y_2, t),$$

can be recast as a non-canonical Hamiltonian system of the form

$$\frac{d}{dt}y_1 = \frac{1}{J}\frac{\partial H}{\partial y_2}(y_1, y_2, t),$$
$$\frac{d}{dt}y_2 = -\frac{1}{J}\frac{\partial H}{\partial y_1}(y_1, y_2, t),$$

where $J = \det D\phi_{1,y}$. This can be done if and only if $divJ(\tilde{F}_1, \tilde{F}_2) = 0$. This holds because $divJ\tilde{F} = JdivF(x,t) = 0$ by volume preservation. Moreover, the fact that w preserves volume, implies

$$\frac{1}{J}\left(\frac{\partial J\xi_1}{\partial y_1} + \frac{\partial J\xi_2}{\partial y_2} + \frac{\partial J\xi_3}{\partial y_3}\right) = 0.$$

But since $\xi_1 = \xi_2 = 0$, $\xi_3 = 1$ one has $\frac{\partial J}{\partial y_3} = 0$. Finally, since $\frac{\partial J\tilde{F}_3}{\partial y_3} = J\frac{\partial F_3}{\partial y_3} + F_3\frac{\partial J}{\partial y_3}$ and $\tilde{F}_3$ does not depend on y_3 we conclude that $divJ\tilde{F} = divJ(\tilde{F}_1, \tilde{F}_2) = 0$.

4. One applies the Darboux theorem, see section 2 to show the existence of coordinates for which one obtains a canonical structure.

□

Remark 1.7. The coordinates in which the vector field takes the form of the new system do not depend on the explicit form of the original vector field. Rather, they depend only on the volume-preserving spatial symmetry group.

[2] We recall that the Lie derivative of a function g with respect to a vector field X in a point x_0 is

$$L_X f(x_0) = \lim_{t \longrightarrow 0} \frac{g(\phi(t; t_0, x_0)) - f(x_0)}{t},$$

where $\phi(t; t_0, x_0)$ is the flow X.

For the system (1.2), these coordinates correspond to $z_1 = s, z_2 = R$ and $z_3 = \theta$, and $H(s,R) = \varepsilon R^2(1 - s^2 - r^2/4)$. The Michelson system (1.1) does not preserve symmetry and the higher order terms in the equation θ depend on the angle θ itself.

As a consequence of the previous theorem, we conclude that given an autonomous volume preserving system that admits a volume preserving symmetry, there exist a volume preserving change of variables such that the system can be expressed in action-angle-angle variables

$$\begin{aligned} \dot{I} &= 0, \\ \dot{\phi_1} &= \Omega_1(I), \\ \dot{\phi_2} &= \Omega_2(I), \end{aligned}$$

where $I \in \mathbb{R}^+, \phi_1 \in S^1$ and $\phi_2 \in S^1$ or $\mathbb{R}$. For that, one can first transform (z_1, z_2) into the standard action-angle variables $\dot{I} = 0, \dot{\phi_1} = \Omega_1(I)$ and then transform the third variable z_3 into ϕ_2 such that it only depends on I, see [29].

This shows that the phase space of a three-dimensional volume preserving flow with a volume preserving symmetry is foliated by two dimensional tori or cylinders, depending on whether z_3 is defined on $\mathbb{R}$ or S^1.

As we have already mention, the Michelson system (1.1) is a perturbation of a system that can be expressed in coordinates of Theorem 1.6 and, as it is autonomous, it admits a first integral. Moreover, the system (1.2) has one action and two frequencies.

From the same theorem we know that the unperturbed system is foliated by two dimensional tori. In section 3.5 we will conclude that some of theses tori persist for the Michelson flow for small values of ε.

Chapter 2

Local reduction of a volume-preserving flow to a canonical area-preserving map

In this chapter we will proof that the reduction of a volume preserving flow to a Poincaré map preserves an area form. This area form could not be the canonical one. We include Darboux's theorem that asserts that all symplectic forms are locally equivalent, allowing to consider canonical area preserving maps for local properties of the dynamics. The presented proof of the Darboux theorem uses the so-called Moser's trick, some background on differential forms is also briefly include. Using a Poincaré map for the Michelson system we describe aspects on the local dynamics of area preserving maps.

2.1 Reduction of a VPF to an APM

One of the methodologies that one can use to describe the topology of the phase space of a three dimensional flow is to use a Poincaré map to study the behaviour of the system. We remark that in general, this cannot be done globally, but only where a suitable transverse section exists. Different sections can be used to investigate different aspects of the dynamics. Here we shall see that in any transverse section, where the dynamics is recurrent, the Poincaré preserves a suitable 2-form.

Let $X : U \subset \mathbb{R}^3 \longrightarrow \mathbb{R}^3$ be a three dimensional vector field $\mathcal{C}^r, r \geqslant 1$ such that the associated flow φ_t preserves the standard volume form $\Omega = dx \wedge dy \wedge dz$. That is, for all $x_0 \in U$ and for all $u_1, u_2, u_3 \in \mathbb{R}^3$,

$$\Omega_{\varphi(t,x_0)}(D_{x_0}\varphi(t,x_0)u_1, D_{x_0}\varphi(t,x_0)u_2, D_{x_0}\varphi(t,x_0)u_3) = \Omega_{x_0}(u_1,u_2,u_3), \qquad \forall t \in I(x_0) \subset \mathbb{R}.$$

where $I(x_0)$ is the interval of definition of the solution $\varphi(t, x_0)$.

Let Σ be a transverse section and define the Poincaré map $P : \Sigma \longrightarrow \Sigma$, which we assume that is well defined since we have a recurrence property. Given $x \in \Sigma$ and $u_1, u_2 \in T_x\Sigma \subset$

$\mathbb{R}^3$, we define

$$\Omega_x^\Sigma(u_1, u_2) := \Omega_x(X(x), u_1, u_2).$$

Remark 2.1. Since Ω_x is a non-degenerate volume form, also Ω_x^Σ is a volume form. Since Σ is a transverse section, then Ω_x^Σ in non-degenerated.

Theorem 2.2. *The Poincaré map $P : \Sigma \longrightarrow \Sigma$ preserves the differential 2-form Ω^Σ.*

Proof. One can parametrize Σ as the image of a ball B, $\Sigma = \nu(B)$ where $\nu : B \subset \mathbb{R}^3 \longrightarrow \mathbb{R}^3$ is a $\mathcal{C}^r$ injective immersion.
Let $s \in B$ such that $x = \nu(s)$ and $v_1, v_2 \in \mathbb{R}^2$ such that

$$u_1 = D\nu(s)v_1, \qquad u_2 = D\nu(s)v_2.$$

We want to prove that P preserves the differential 2-form Ω^Σ,

$$\Omega^\Sigma_{P(x)}(DP(x)u_1, DP(x)u_2) = \Omega^\Sigma_x(u_1, u_2).$$

Since P can be expressed as $P(x) = \nu(\bar{P}(\nu^{-1}(x))) = \nu(\bar{P}(s))$ for $\bar{P} : B \longrightarrow B$, we have that

$$\begin{aligned} DP(x)u_1 &= D\nu(\bar{P}(s))D\bar{P}(s)D\nu^{-1}(x)u_1 = D\nu(\bar{P}(s))D\bar{P}(s)D\nu^{-1}(x)D\nu(s)v_1 \\ &= D(\nu \circ \bar{P})(s)D(\nu^{-1} \circ \nu)(s)v_1 = D(\nu \circ \bar{P})(s)v_1. \end{aligned}$$

Analogously, $DP(x)u_2 = D(\nu \circ \bar{P})(s)v_2$. Therefore,

$$\begin{aligned} \Omega^\Sigma_{P(x)}(DP(x)u_1, DP(x)u_2) &= \Omega_{P(x)}(X(P(x)), DP(x)u_1, DP(x)u_2) \\ &= \Omega_{\nu(\bar{P}(s))}(X(\nu(\bar{P}(s))), D(\nu \circ \bar{P}(s)v_1, D(\nu \circ \bar{P}(s)v_2). \end{aligned}$$

Let $\tau : B \longrightarrow \mathbb{R}$ be the return time of $x = \nu(s)$ to the section Σ, i.e. such that $P(x) = \varphi(\tau(s), x)$, or equivalently

$$\nu(\bar{P}(s)) = \varphi(\tau(s), \nu(s)).$$

Therefore

$$\begin{aligned} &\Omega_{\nu(\bar{P}(s))}(X(\nu(\bar{P}(s))), D(\nu \circ \bar{P})(s)v_1, D(\nu \circ \bar{P})(s)v_2) \\ &= \Omega_{\varphi(\tau(s),\nu(s))}(X(\varphi(\tau(s), \nu(s))), D_s\varphi(\tau(s), \nu(s))v_1, D_s\varphi(\tau(s), \nu(s))v_2). \end{aligned}$$

Observe that

$$\begin{aligned} D_s\varphi(\tau(s), \nu(s)) &= D_t\varphi(\tau(s), \nu(s))D_s\tau(s) + D_x\varphi(\tau(s), \nu(s))D_s\nu(s) \\ &= X(\varphi(\tau(s), \nu(s)))D_s\tau(s) + D_x\varphi(\tau(s), \nu(s))D_s\nu(s). \end{aligned}$$

Hence

$$\begin{aligned} D_s\varphi(\tau(s), \nu(s))v_i &= X(\varphi(\tau(s), \nu(s)))D_s\tau(s)v_i + D_x\varphi(\tau(s), \nu(s))D_s\nu(s)v_i \\ &= \lambda_i X(\varphi(\tau(s), \nu(s))) + D_x\varphi(\tau(s), \nu(s))D_s\nu(s)v_i. \end{aligned}$$

and, since Ω is a an alternating multilinear form,

$$\begin{aligned} &\Omega_{\varphi(\tau(s),\nu(s))}(X, \lambda_1 X + D_x\varphi(\tau(s), \nu(s))D_s\nu(s)v_1, \lambda_2 X + D_x\varphi(\tau(s), \nu(s))D_s\nu(s)v_2) \\ &= \Omega_{\varphi(\tau(s),\nu(s))}(X, D_x\varphi(\tau(s), \nu(s))D_s\nu(s)v_1, D_x\varphi(\tau(s), \nu(s))D_s\nu(s)v_2). \end{aligned}$$

Given that X is invariant through the associated flow φ,

$$X(\varphi(\tau(s),\nu(s))) = D_x\varphi(\tau(s),\nu(s))X(\nu(s)),$$

and therefore

$$\begin{aligned}&\Omega_{\varphi(\tau(s),\nu(s))}(X(\varphi(\tau(s),\nu(s))), D_x\varphi(\tau(s),\nu(s))D_s\nu(s)v_1, D_x\varphi(\tau(s),\nu(s))D_s\nu(s)v_2)\\ &= \Omega_{\varphi(\tau(s),\nu(s))}(D_x\varphi(\tau(s),\nu(s))X(\nu(s)), D_x\varphi(\tau(s),\nu(s))D_s\nu(s)v_1, D_x\varphi(\tau(s),\nu(s))D_s\nu(s)v_2).\end{aligned}$$

As $\varphi(\tau(s),\nu(s)) = P(x)$ preserves the volume form, we have

$$\begin{aligned}&\Omega_{\varphi(\tau(s),\nu(s))}(D_x\varphi(\tau(s),\nu(s))X(\nu(s)), D_x\varphi(\tau(s),\nu(s))D_s\nu(s)v_1, D_x\varphi(\tau(s),\nu(s))D_s\nu(s)v_2)\\ &= \Omega_{P(x)}(DP(x)X(x), DP(x)u_1, DP(x)u_2) = \Omega_x(X(x),u_1,u_2) = \Omega^{\Sigma}_x(u_1,u_2).\end{aligned}$$

So we have proved that P preserves the differential 2-form Ω^{Σ}.

□

2.2 Darboux theorem

Given any two symplectic forms, Darboux's theorem gives the existence of a change of coordinates that locally relates both forms. Indeed, this change of coordinates is used in the last step of the proof of Theorem 1.6, to get the standard form. In other words, Darboux theorem states that all symplectic structures are locally equivalent.

Definition 2.3. Let V a linear vector space. A real *symplectic form* $\omega : V \times V \longrightarrow \mathbb{R}$ is an antisymmetric and non-degenerate bilinear form. That is, $\omega(v,v) = 0$ for all $v \in V$, and if $\omega(v,w) = 0$ for all $v \in V$, then $w = 0$.

Definition 2.4. The *interior product* of a k-form ω is the $(k-1)$-form defined by

$$i_X\omega(v_1,\ldots,v_{k-1}) = \omega(X, v_1,\ldots,v_{k-1}),$$

for any vector fields $v_1,\cdots,v_{k-1}$.

The following formulation of Darboux's theorem is inspired in references [16].

Theorem 2.5 (Darboux)**.** *Let ω be a closed symplectic form on a $2n$-dimensional differentiable manifold M. Then for any $p \in M$ there is a neighbourhood U of p and a diffeomorphism $\phi : U \longrightarrow \mathbb{R}^{2n}$ such that*

$$\phi^*\left(\sum_{i^1}^{n} dx_i \wedge dy_i\right) = \omega,$$

where ϕ^* denote the pullback by ϕ and x_i, y_i are the standard coordinates on $\mathbb{R}^{2n}$.

Proof. Note that it suffices to prove the theorem for $p = 0 \in \mathbb{R}^{2n}$. One can use a coordinate chart to push ω forward to a symplectic form on a neighbourhood of 0. If the result holds on $\mathbb{R}^{2n}$, one can compose the coordinate chart with ϕ and get the theorem in general.

Let $\omega_0 = \sum_{i=1}^{n} dx_i \wedge dy_i$. Since ω is a non-degenerate closed two-form, on the tangent space $T_0\mathbb{R}^{2n}$ it is a non-degenerate anti-symmetric bilinear form. Thus by a linear change of coordinates, $\omega(0)$ can be put in the standard form, so we may assume that $\omega(0) = \omega_0(0)$.

We want to construct a diffeomorphism ϕ such that $\phi^*\omega_0 = \omega$, where ϕ^* denotes the pullback of ϕ, that is $\phi^*\omega_0(v_1, v_2) = \omega(D\phi(v_1), D\phi(v_2))$, for all $v_1, v_2 \in V$.

We shall obtain ϕ by applying the so-called Moser's trick, [16]. The idea is the following. We shall look for a suitable smooth non-autonomous vector field $X(t, x)$ such that if $\phi_t := \phi(t; \cdot, \cdot)$, where ϕ is the evolutionary process, defined on an open domain $D \subset \mathbb{R} \times \mathbb{R} \times \mathbb{R}^n$, associated to the differential equation

$$\dot{x} = X(t, x),$$

verifies

$$\phi_t^* \omega_t = \omega, \tag{2.1}$$

being ω_t the family of 2-forms,

$$\omega_t = t\omega_0 + (1 - t)\omega.$$

Then the diffeomorphism ϕ will be ϕ_1.
We differentiate (2.1) to see which conditions X_t has to verify, and we get

$$0 = \frac{d}{dt}\phi_t^*\omega_t = (\frac{d}{dt}\phi_t^*)\omega_t + \phi_t^* \frac{d}{dt}\omega_t.$$

Let $L_{X_t}\omega = \frac{d}{dt}|_{t=0}(\phi_t^*\omega)$ be the Lie derivative of ω_t with respect to the vector field X_t. Then one can compute the derivative $\frac{d}{ds}\phi_s^*\omega$, applying $s \longmapsto s + t$ and the chain rule,

$$\left(\frac{d}{ds}\phi_s^*\right)\omega = \left(\frac{d}{dt}|_{t=0}\phi_{t+s}^*\right)\omega = \phi_t^* \frac{d}{dt}|_{t=0}\left(\phi_s^*\right)\omega = \phi_s^* L_{X_t}\omega.$$

Thus $(\frac{d}{dt}\phi_t^*)\omega_t + \phi_t^* \frac{d}{dt}\omega_t = \phi_t^*(L_{X_t}\omega_t + \omega_0 - \omega) = 0$.
We apply Cartan's identity, $L_{X_t}\omega_t = d\iota_{X_t}\omega_t + \iota_{X_t}d\omega_t$, where ι_{X_t} is the interior product and d denotes the exterior derivative. We refer to [3] for definitions and proofs. Thus

$$0 = \phi_t^*(d\iota_{X_t}\omega_t + \omega_0 - \omega),$$

since ω_t is closed (that is, $d\omega_t = 0$), because it is a linear combination of ω and ω_0 that are closed.

By Poincaré's Lemma,[3] which states that any closed differential form defined on a simply connected domain on M is exact, $\omega_0 - \omega$ is locally exact, so we can write $\omega_0 - \omega = d\lambda$, where λ is a 1-form, and thus $0 = d(\iota_{X_t}\omega_t + \lambda)$.
Given ω a non-degenerated volume form there exist a vector X, such that for any $v \in V$ it satisfies the equation $\omega(X, v) = -\lambda(v)$. Hence $\iota_X\omega = -\lambda$. This provides that for any t, there is vector X_t such that $\iota_{X_t}\omega_t = -\lambda$. Hence this condition defines the non-autonomous vector field [1].

[1]Note that $\omega_t = \omega_0$ at 0, so ω_t will be non-degenerate on an open neighbourhood of 0, since ω_0 is non-degenerate.

Since $\omega(0) = \omega_0(0)$, we have that $\lambda = 0$ and thus $X_t(0) = 0$ for all $t \in \mathbb{R}$. This means that $\phi(t; t_0, 0) = 0$ for all t. Thus, by continuity of the solution of the Cauchy problem with respect to the initial condition, which implies the continuous dependence of the interval of definition of the solution of the Cauchy problem, we can choose a sufficiently small neighbourhood of 0, the flow ϕ_t will be defined for time greater than 1. In this neighbourhood, $\phi = \phi_1$ gives the desired result.

□

2.3 A Poincaré map for the Michelson system

The geometrical properties of the Michelson system described above, and concretely, the fact that it is a perturbation of a system with rotational symmetry (1.3), motivates to consider a section $\Sigma = \{z = 0\}$. Since $T_p\Sigma = \langle (1,0,0), (0,1,0) \rangle$ for all $p \in \Sigma$, the subspace $\langle (0,0,1) \rangle$ is orthogonal to $T_p\Sigma$. Then $F_\varepsilon(p) \cdot (0,0,1) = \varepsilon(1-x^2) - y$ which vanishes on the parabola $y = \varepsilon(1-x^2)$. Outside a neighbourhood of the parabola, Σ defines a transverse section. As expected, this parabola is a perturbation of the rotation axis of the elements of the Lie group G of symmetries of the averaged system (1.2).

Given the Michelson system (1.1) we compute the differential 2-form Ω^Σ for $\Sigma \equiv \{z = 0\}$. Σ is a local Poincaré section of the system, that loose the transverse condition near the x axis.

$$\Omega^\Sigma_{(x,y,0)}(u_1,u_2) = \Omega_{(x,y,0)}(X(x,y,0),u_1,u_2) = \begin{vmatrix} y & u_{11} & u_{21} \\ 0 & u_{12} & u_{22} \\ \varepsilon(1-x^2)-y & 0 & 0 \end{vmatrix}$$
$$= (\varepsilon(1-x^2)-y) \begin{vmatrix} u_{11} & u_{21} \\ u_{12} & u_{22} \end{vmatrix} = (\varepsilon(1-x^2)-y) dx \wedge dy.$$

The area form of the Michelson flow depends on the function of $\varepsilon(1-x^2) - y$ so it does not preserves the standard area form. We will see that the associated Poincaré map of the Michelson system can be locally reduced to a map that preserves the standard area form.

To compute the Poincaré map, we have implemented a Taylor method with variable step size to integrate the Michelson system (1.1). Given an initial condition, we compute the image of the Poincaré map $P_\varepsilon : \Sigma \longrightarrow \Sigma$, integrating the system until we find two points z_k and z_{k+1} such that $z_k z_{k+1} < 0$. Thus we use a Newton method to determine a step size h that gives a point of the orbit on Σ. We refer to [35] for an explanation of these numerical algorithms. Also [22] is a good reference for the Taylor method [2].

In Figure 2.1 we display the phase space of the Poincaré map for different values of the parameter ε. By the previous results, P_ε is non-canonical area preserving map. In the figure we see a set of invariant curves on $y > 0$ that surround an elliptic fixed point. Since the system is a perturbation of a symmetry with a rotational symmetry around the x axis,

[2] We have not used the Taylor package nor any other package, implementations where done in C and adapted when required to PARI/GP, [10].

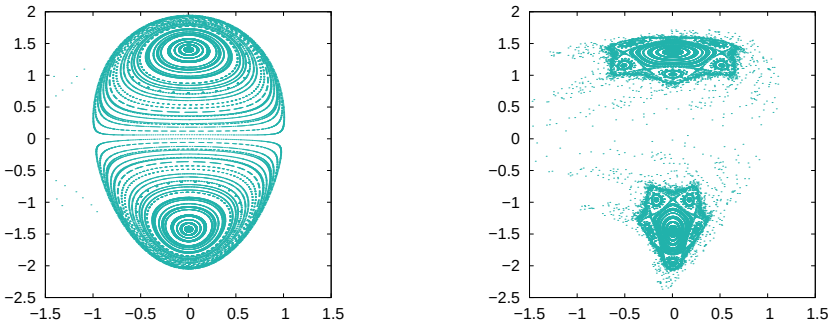

Figure 2.1: Poincaré section of the Michelson flow for $\varepsilon = 0.0316$ and 0.1405.

we observe a similar structure for $y < 0$. Later on we will see how to compute these fixed points as well as their linear behaviour as a function of ε, see section 3.2.
The elliptic fixed points are the intersections with Σ of an elliptic periodic orbit of the Michelson system (1.1). Similarly, the intersection with Σ of an invariant torus of the flow is seen in the Poincaré section as two invariant curves, one for $y > 0$ and the other for $y < 0$.

As observed in section 1.1, the saddle focus fixed points of the Michelson system $(\pm 1, 0, 0)$ have one dimensional and two dimensional invariant manifolds that nearly coincide when ε tends to 0. Accordingly, one can see in the left plot that the intersection of the two dimensional manifolds with Σ encloses the tori around the elliptic fixed point.
For $\varepsilon > 0$, the system looses the rotational symmetry and is no longer integrable. In general, for a non-integrable system one expects that the invariant manifolds do not coincide. We will compute these invariant manifolds in section 4.1. As will be shown the two-dimensional invariant manifolds intersect transversely while the one-dimensional invariant manifolds do not intersect and one rotates around the other one.
On the other hand, on the right figure, we see invariant curves for larger values of ε. Moreover, for the value of ε considered in the plot, we clearly observe elliptic 5-periodic orbit of P_ε. Around the 5-periodic orbits, there is a set of invariant curves that forms an island. At the places where the islands approach, there is a 5-periodic hyperbolic orbit. This structure is a consequence of the Poincaré-Birkhoff Theorem that will be detailed in section 3.4.

The transverse intersection of the invariant manifolds of the 5-periodic hyperbolic orbit generates chaos in phase space. The chaotic regions can be contained inside the stability domain, hence giving rise to a confined regions of chaos, or can be open chaotic regions. In Figure 2.3 left we illustrate a confined chaotic region related to the 5-periodic orbit while in the right plot we see that there are no invariant curves surrounding the 5-periodic islands and points near the 5-periodic hyperbolic orbit escape when iterating the Poincaré map.

All the previous concepts and statement about invariant curves and resonant islands of P_ε need to be properly justified. They rely on the intrinsic properties of the dynamics of area preserving maps around elliptic fixed points. These properties are revealed when

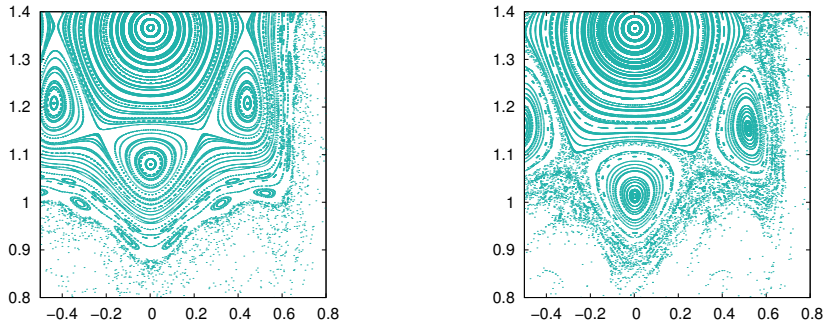

Figure 2.2: Zoom on an island of the Poincaré map for $\varepsilon = 0.138$ and $\varepsilon = 0.1405$.

transforming the map to a normal form, as we will see in the next section.
From now on, we will study an area preserving map locally around an elliptic fixed point. Hence, without loss of generality, we will assume that it preserves the standard form since Darboux's theorem reduces any symplectic form to a canonical form.

Chapter 3

Birkhoff normal form of an area-preserving map around an elliptic fixed point

This chapter aims to study the dynamics of area preserving maps around elliptic fixed points by turning the map into a Birkhoff normal form. For that, we will use symplectic changes of coordinates, defined as the time-one flow of a Hamiltonian, to assure that the Birkhoff normal form is still an area preserving map.
Moreover, we will study the phase space of a truncated Birkhoff normal form, using the fact that it is an area preserving twist map and, finally, we will do some comments on the persistence of invariant objects when perturbing the system.

3.1 Birkhoff normal form of an APM

The aim of this section is to introduce the Birkhoff normal form of F, which allow us to study the local dynamics around the fixed point. We will see that F cannot be linearized by a change of coordinates and some terms cannot be removed.

Definition 3.1. We define the *set of resonances* as the set $\Gamma = \{k \in \mathbb{Z} : k\alpha = 0 \mod 1\}$. The resonance $k = 0$ is the so-called unavoidable resonance. Resonances $k \neq 0$ are avoidable resonances.

The terms that cannot be removed correspond to resonances and will be referred as resonant terms. If $z = x + iy$, a term $z^k\bar{z}^l$ of the first component (respectively the second), of F is resonant if $k - l - 1 = 0$ (respectively if $k - l + 1 = 0$).

As shown in the previous chapter, the Poincaré map of a volume preserving flow is an area preserving map, denoted as F, with an elliptic fixed point that corresponds to the elliptic periodic orbit of the flow. Given the fixed point $p \in \mathbb{R}^2$, $DF(p)$ has two eigenvalues $\lambda, \bar{\lambda} \in \mathbb{C}$ such that $\lambda = e^{2\pi i\alpha}$ with $\alpha \in (0,1)$. Thus $DF(p)$ can be expressed as a rotation, $DF(p) = R_\alpha$, after a linear change of coordinates.

Definition 3.2. A map F is said to be in *Birkhoff normal form* around a fixed point p if and only if it commutes with the semi simple part of DF at p.

The following theorem assures the existence of a change of variables that allow us to construct the Birkhoff normal form of F around an elliptic fixed point. We refer to [2]. The changes we use are canonical and expressed as the time-one map of a Hamiltonian, using Lie series as explained in [28].

Theorem 3.3. *Given an area preserving map $F : \mathbb{R}^2 \longrightarrow \mathbb{R}^2$ there exists a formal canonical change of variables $\phi : \mathbb{R}^2 \longrightarrow \mathbb{R}^2$ in a neighbourhood of an elliptic fixed point such that F is in Birkhoff normal form around the fixed point in the new coordinates. That is, $N = \phi \circ F \circ \phi^{-1}$ satisfies $N \circ DF = DF \circ N$.*

Proof. We will consider $F : \mathbb{C}^2 \longrightarrow \mathbb{C}^2$ in complex variables $z, \bar{z}$ given by the change of variables $z = x + iy$ and $\bar{z} = x - iy$. The eigenvalues of $DF(z_0)$ are then $\lambda = e^{2\pi i\alpha}$ and $\bar{\lambda}$, where $\alpha \in (0,1)$ is the multiplier at the fixed point $z_0 \in \mathbb{C}^2$.

We can express F as a sum of homogeneous polynomials of degree $r = k + l$. Since the map F is real, the second component is conjugated to the first one $F = (f, \bar{f})$, hence we can consider just one of them,

$$f(z,\bar{z}) = \lambda z + \sum_{r \geqslant 2} c_{kl} z^k \bar{z}^l = \lambda z + g(z,\bar{z}).$$

We aim to find the change of coordinates ϕ constructed as a sequence of transformations which successively remove the non-linear terms. Moreover, we will consider a symplectic change of coordinates to assure that the Birkhoff normal form still preserves the area form. In particular, we will construct a canonical change of variables as a time 1-map of an autonomous canonical real Hamiltonian system with Hamiltonian $X(x,y)$.

$$(x,y) \longmapsto \phi_X^1(x,y),$$

where ϕ_X^t denotes the corresponding flow.
Since X is Hamiltonian, it can be expressed as $\dot{x} = \frac{\partial X}{\partial y}, \dot{y} = -\frac{\partial X}{\partial x}$ and doing a change of coordinate $z = x + iy$, $\bar{z} = x - iy$, we get

$$\begin{cases} \dot{z} = -2i\frac{\partial X}{\partial \bar{z}} \\ \dot{\bar{z}} = 2i\frac{\partial X}{\partial z} \end{cases}$$

which are the equations of motion of the Hamiltonian flow X in coordinates $z, \bar{z}$.
We use the Taylor expansion with respect to time to find the solution at time $t = 1$,

$$z(t) = z(0) + \frac{dz}{dt}(0)t + \frac{d^2z}{dt^2}(0)\frac{t^2}{2} + \frac{d^3z}{dt^3}(0)\frac{t^3}{3!} + \cdots$$

Thus we need to find the n-th derivative of z. If $h(z,\bar{z}) := \dot{z} = -2i\frac{dX}{d\bar{z}}$, then

$$\ddot{z} = \frac{\partial h}{\partial z}\dot{z} + \frac{\partial h}{\partial \bar{z}}\dot{\bar{z}} = \frac{\partial h}{\partial z}\left(-2i\frac{\partial X}{\partial \bar{z}}\right) + \frac{\partial h}{\partial \bar{z}}\left(2i\frac{\partial X}{\partial z}\right) = 2i\left(\frac{\partial h}{\partial \bar{z}}\frac{\partial X}{\partial z} - \frac{\partial h}{\partial z}\frac{\partial X}{\partial \bar{z}}\right) = 2i\{X,h\}.$$

Thus, denoting by $L_X(h) = 2i\{X, h\}$, where $\{X, h\}$ is the Lie bracket, we find recursively

$$\begin{aligned}
\dot{z} &= -2i\frac{\partial X}{\partial \bar{z}} = 2i\left(\frac{\partial z}{\partial \bar{z}}\frac{\partial X}{\partial z} - \frac{\partial z}{\partial z}\frac{\partial X}{\partial \bar{z}}\right) = L_X(z),\\
\ddot{z} &= L_X(h) = L_X(L_X(z)) = L_X^2(z),\\
&\vdots\\
z^{(n)} &= L_X^n(z).
\end{aligned}$$

Since $z(0) = z$, we get

$$z(1) = z + L_X(z) + \frac{1}{2}L_X^2(z) + \frac{1}{3!}L_X^3(z) + \cdots = \sum_{k=0}^{\infty}\frac{L_X^k(z)}{k!} = e^{L_X(z)}.$$

Analogously, $\bar{z}^{(n)} = L_X^n(\bar{z})$ and thus

$$\bar{z}(1) = \bar{z} + L_X(\bar{z}) + \frac{1}{2}L_X^2(\bar{z}) + \frac{1}{3!}L_X^3(\bar{z}) + \cdots = \sum_{k=0}^{\infty}\frac{L_X^k(\bar{z})}{k!} = e^{L_X(\bar{z})}.$$

Therefore the time 1-map of the Hamiltonian flow X is $\phi_X^1 = e^{L_X}Id$.

Let X_{p+1} be an homogeneous vector field of degree $p+1$. We will construct the change of coordinates ϕ as a composition of canonical changes $\phi^1_{X_{p+1}}(z, \bar{z})$ that attempts to remove the corresponding non-linear term of order p from F.

Assuming that F is in Birkhoff normal form up to order $p-1$, we aim to remove the term of order p using the change of coordinates $\phi^1_{X_{p+1}}(z, \bar{z})$. That is, the term of order p of $N(z, \bar{z}) = \phi^1_{X_{p+1}} \circ F \circ \phi^{-1}_{X_{p+1}}(z, \bar{z})$ should be zero.

Using the change of coordinates

$$\phi^1_{X_{p+1}}(z, \bar{z}) = e^{L_{X_{p+1}}}(z, \bar{z}) = (z - 2i\frac{\partial X_{p+1}}{\partial \bar{z}}(z, \bar{z}), \bar{z} + 2i\frac{\partial X_{p+1}}{\partial z}(z, \bar{z})) + \mathcal{O}_{p+1},$$

and

$$\phi^{-1}_{X_{p+1}}(z, \bar{z}) = (z + 2i\frac{\partial X_{p+1}}{\partial \bar{z}}(z, \bar{z}), \bar{z} - 2i\frac{\partial X_{p+1}}{\partial z}(z, \bar{z})) + \mathcal{O}_{p+1},$$

one obtains

$$\begin{aligned}
N(z, \bar{z}) &= \phi^1_{X_{p+1}} \circ F \circ \phi^{-1}_{X_{p+1}}(z, \bar{z}) = \phi^1_{X_{p+1}} \circ F\left(\left(z + 2i\frac{\partial X_{p+1}}{\partial \bar{z}}(z, \bar{z}), \bar{z} - 2i\frac{\partial X_{p+1}}{\partial z}(z, \bar{z})\right) + \mathcal{O}_{p+1}\right)\\
&= \phi^1_{X_{p+1}}\left(F(z, \bar{z}) + \left(2i\lambda\frac{\partial X_{p+1}}{\partial \bar{z}}, -2i\bar{\lambda}\frac{\partial X_{p+1}}{\partial z}\right)(z, \bar{z}) + \mathcal{O}_{p+1}\right)\\
&= F(z, \bar{z}) + \left(2i\lambda\frac{\partial X_{p+1}}{\partial \bar{z}}, -2i\bar{\lambda}\frac{\partial X_{p+1}}{\partial z}\right)(z, \bar{z}) + \left(-2i\frac{\partial X_{p+1}}{\partial \bar{z}}, 2i\frac{\partial X_{p+1}}{\partial z}\right)(\lambda z, \bar{\lambda}\bar{z}) + \mathcal{O}_{p+1}.
\end{aligned}$$

Considering just the term of order p, this leads to the homological equation

$$\frac{1}{2i}F_p = \left(\lambda\frac{\partial X_{p+1}}{\partial \bar{z}} - \frac{\partial X_{p+1}}{\partial \bar{z}}(\lambda z, \bar{\lambda}\bar{z}), -\bar{\lambda}\frac{\partial X_{p+1}}{\partial z} + \frac{\partial X_{p+1}}{\partial z}(\lambda z, \bar{\lambda}\bar{z})\right).$$

where F_p denotes the term of order p of F.

Since X_{p+1} is an homogeneous vector field of order $p+1$,

$$\frac{\partial X_{p+1}}{\partial \bar{z}}(\lambda z, \bar{\lambda}\bar{z}) = \sum_{k+l=p} \lambda^k \bar{\lambda}^l \frac{\partial X_{p+1}}{\partial \bar{z}}(z, \bar{z}),$$

we get that the homological equation for the first component is

$$\frac{1}{2i} f_p = \lambda \frac{\partial X_{p+1}}{\partial \bar{z}} - \sum_{k+l=p} \lambda^{k-l} \frac{\partial X_{p+1}}{\partial \bar{z}} = \left(\lambda - \sum_{k+l=p} \lambda^{k-l}\right) \frac{\partial X_{p+1}}{\partial \bar{z}}.$$

If there exists k, l such that $k+l=p$ and $\lambda = \lambda^{k-l}$, this equation cannot be satisfied and so the term of order p cannot be removed. Hence the unavoidable resonant terms, see definition 3.1 with $k = l+1$ should be kept.

Let f_p^{nr} denote the non-resonant terms of order p of the first component of F and then the homological equation is given by

$$\frac{1}{2i} f_p^{nr} = \lambda \frac{\partial X_{p+1}}{\partial \bar{z}} - \frac{\partial X_{p+1}}{\partial \bar{z}}(\lambda z, \bar{\lambda}\bar{z}). \tag{3.1}$$

We want to prove that this equation has a real solution to get a vector field X_p, which allow us to construct the change of coordinates. For that, we will use that F is an area preserving map. Since the second component of F is conjugated to the first one, we compute the area form as $df \wedge d\bar{f}$,

$$\begin{aligned} df \wedge d\bar{f} &= (\lambda dz + \frac{\partial g}{\partial z} dz + \frac{\partial g}{\partial \bar{z}} d\bar{z}) \wedge (\bar{\lambda} d\bar{z} + \frac{\partial \bar{g}}{\partial \bar{z}} d\bar{z} + \frac{\partial \bar{g}}{\partial z} dz) \\ &= \lambda dz \wedge \bar{\lambda} d\bar{z} + \lambda dz \wedge \frac{\partial \bar{g}}{\partial \bar{z}} d\bar{z} + \frac{\partial g}{\partial z} dz \wedge \bar{\lambda} d\bar{z} + \frac{\partial g}{\partial z} dz \wedge \frac{\partial \bar{g}}{\partial \bar{z}} d\bar{z} + \frac{\partial g}{\partial \bar{z}} d\bar{z} \wedge \frac{\partial \bar{g}}{\partial z} dz \\ &= \left(1 + \lambda \frac{\partial \bar{g}}{\partial \bar{z}} + \bar{\lambda} \frac{\partial g}{\partial z} + \frac{\partial g}{\partial z}\frac{\partial \bar{g}}{\partial \bar{z}} - \frac{\partial g}{\partial \bar{z}}\frac{\partial \bar{g}}{\partial z}\right) dz \wedge d\bar{z}. \end{aligned}$$

Since F is area preserving, we have that $df \wedge d\bar{f} = dz \wedge d\bar{z}$ and thus

$$\lambda \frac{\partial \bar{g}}{\partial \bar{z}} + \bar{\lambda} \frac{\partial g}{\partial z} + \frac{\partial g}{\partial z}\frac{\partial \bar{g}}{\partial \bar{z}} - \frac{\partial g}{\partial \bar{z}}\frac{\partial \bar{g}}{\partial z} = 0.$$

This is equivalent to $2Re(\bar{\lambda}\frac{\partial g}{dz}) - \{g, \bar{g}\} = 0$. Taking terms of order $p-1$ we have that,

$$2Re(\bar{\lambda}\frac{\partial g_p}{dz}) = \sum_{k \geqslant 2} \{\bar{g}_k, g_{p-k+1}\}.$$

Suppose f is in normal form up to order $p-1$, the non-resonant terms g_p^{nr} of order p satisfy $2Re(\bar{\lambda}\frac{\partial g_p^{nr}}{dz}) = 0$ and hence there exists h real such that $\bar{\lambda} g_p^{nr} = -2i\frac{\partial h}{\partial \bar{z}}$. This can be easily proved considering $h(z,\bar{z}) = \frac{-1}{2i}\int_0^{\bar{z}} \bar{\lambda} g_p^{nr}(z,s)ds + cz^{p+1}$, such that we have

$Re(\frac{\partial \bar{\lambda} g_p^{nr}}{\partial z}) = Re(-2i\frac{\partial^2 h}{\partial \bar{z}\partial z}) = -2Im(\frac{\partial^2 h}{\partial \bar{z}\partial z}) = 0$ if and only if h is real.

Then to prove the existence of a real solution of (3.1), we let $h(z,\bar{z}) = X_{p+1}(\lambda z, \bar{\lambda}\bar{z}) - X_{p+1}(z,\bar{z}) + \frac{1}{2i}z\bar{z}$ such that

$$\bar{\lambda} g_p^{nr} = -2i\frac{\partial h}{\partial \bar{z}} = -2i\bar{\lambda}\frac{\partial X_{p+1}}{\partial \bar{z}}(\lambda z, \bar{\lambda}\bar{z}) + 2i\frac{\partial X_{p+1}}{\partial \bar{z}}(z,\bar{z}) - z.$$

Thus we have that

$$g_p^{nr} = -2i\frac{\partial X_{p+1}}{\partial \bar{z}}(\lambda z, \bar{\lambda}\bar{z}) + 2i\lambda\frac{\partial X_{p+1}}{\partial \bar{z}}(z,\bar{z}) - \lambda z.$$

This is equivalent to

$$f_p^{nr} = \lambda z + g_p^{nr} = -2i\frac{\partial X_{p+1}}{\partial \bar{z}}|_{(\lambda z, \bar{\lambda}\bar{z})} + 2i\lambda\frac{\partial X_{p+1}}{\partial \bar{z}}(z,\bar{z}),$$

so that the equation (3.1) has a real solution. Therefore we can construct a sequence of change of variables $\phi^1_{X_{p+1}}$ that removes all the non-resonant terms of order p from f.

This process can be carried out up to the desired order or, at a formal level, up to any order. Hence the complete sequence of changes reduces the original map to the desired normal form having only the resonant terms. Each resonant monomial commutes with $diag(\lambda, \bar{\lambda})$.

□

The sequence of analytic changes used to prove the previous theorem, is generically non-convergent, meaning that the width of the domain of analyticity of the transformed map, reduces after each change, and tends to zero. This implies that beyond all orders phenomena, like the exponentially small splitting of separatrices, rely on analytic properties and cannot be captured by the normal form. However one can use the normal form up to a suitable order, to obtain a detailed description of the phase space in a suitable region around the fixed point. For example, a truncated normal form, allows to get a detailed description of the phase space around resonances of F. In the following we illustrate how to use the truncated normal form to get such description.

Assume that the eigenvalues of F at a fixed point, are of the form $\lambda = e^{\pm 2\pi i\alpha}$ with $\alpha = \frac{q}{m} + \delta$ and δ sufficiently small to be close to the resonance of order m, that is such that $\lambda^m \approx 1$. Thus the corresponding term cannot be removed to assure the existence of a relatively large domain, uniform for δ close to zero, where a good model could be obtained.

Therefore the first component of Birkhoff normal form of F up to order m can be expressed in terms of $(z,\bar{z})$ as

$$BNF_m(z,\bar{z}) = \lambda z + a_1 z^2\bar{z} + \cdots + a_s z^{s+1}\bar{z}^s + \tilde{c}\bar{z}^{m-1} + \tilde{\mathcal{R}}_{m+1}(z,\bar{z}),$$

where $a_i \in \mathbb{C}$ and s is the integer part of $\frac{m-1}{2}$. If $r^2 = z\bar{z}$ then

$$\begin{aligned} BNF_m(z,\bar{z}) &= \lambda z + \sum_{j=1}^{s} a_j z^{j+1}\bar{z}^j + \tilde{c}\bar{z}^{m-1} + \tilde{\mathcal{R}}_{m+1}(z,\bar{z}) \\ &= \lambda z(1 + \sum_{j=1}^{s} \lambda^{-1} a_j r^{2j}) + \tilde{c}\bar{z}^{m-1} + \tilde{\mathcal{R}}_{m+1}(z,\bar{z}) \\ &= R_{2\pi q/m}\left(e^{2\pi i\delta} z(1 + \sum_{j=1}^{s} \lambda^{-1} a_j r^{2j}) + e^{-2\pi i q/m}\tilde{c}\bar{z}^{m-1}\right) + \tilde{\mathcal{R}}_{m+1}(z,\bar{z}). \end{aligned}$$

To express $1 + \sum_{j=1}^{s} \lambda^{-1} a_j r^{2j}$ in terms of the so-called Birkhoff coefficients, we use the Taylor series of the logarithm $\ln(1+w) = \sum_{n=1}^{\infty} (-1)^{n+1} \frac{w^n}{n}$, where $w = \sum_{j=1}^{s} \lambda^{-1} a_j r^{2j}$.

To compute $w^n = \left(\sum_{j=1}^{s} \lambda^{-1} a_j r^{2j}\right)^n$, for $n \geqslant 2$ we use that

$$(x_1 + x_2 + \cdots + x_m)^n = \sum_{k_1+k_2+\cdots+k_m=n} \binom{n}{k_1, k_2, \cdots, k_m} \prod_{1 \leqslant t \leqslant m} x_t^{k_t}.$$

Thus

$$\begin{aligned} w^n &= \lambda^{-n}(a_1 r^2 + \cdots a_s r^{2s})^n = \lambda^{-n} \sum_{k_1+k_2+\cdots+k_s=n} \frac{n!}{k_1! \cdots k_s!} (a_1 r^2)^{k_1} \cdots (a_s r^{2s})^{k_s} \\ &= \lambda^{-n} \sum_{k_1+k_2+\cdots+k_s=n} \frac{n!}{k_1! \cdots k_s!} (a_1)^{k_1} \cdots (a_s)^{k_s} r^{2k_1+\cdots+2sk_s} = \sum_{k_1+k_2+\cdots+k_s=n} \lambda^{-n} C_n r^{2k_1+\cdots+2sk_s}. \end{aligned}$$

Therefore the Taylor expansion of the logarithm is

$$\ln(1+w) = \sum_{n=1}^{\infty} (-1)^{n+1} \frac{w^n}{n} = \sum_{j=1}^{s} \lambda^{-1} a_j r^{2j} + \sum_{n=2}^{\infty} \left(\frac{(-1)^{n+1}}{n} \sum_{k_1+k_2+\cdots+k_s=n} \lambda^{-n} C_n r^{2k_1+\cdots+2sk_s} \right).$$

Rearranging all the terms $r^{2k_1+\cdots+2sk_s}$, and ordering them from r^2 up to r^{2s} we get $2\pi i \sum_{i=1}^{s} b_i r^{2i}$ for some $b_i \in \mathbb{R}$ since all the terms of order greater than $2s$ are moved to $\mathcal{R}_{m+1}(z,\bar{z})$.
Therefore $(1 + \sum_{j=1}^{s} \lambda^{-1} a_j r^{2j}) = e^{\ln(1+\sum_{j=1}^{s} \lambda^{-1} a_j r^{2j})} = e^{2\pi i(b_1 r^2 + b_2 r^4 + \cdots + b_s r^{2s})}$.

Using this relation we can compute the Birkhoff coefficients b_i. The first ones are given by

$$b_1 = \frac{\lambda^{-1} a_1}{2\pi i}, \qquad b_2 = \frac{1}{2\pi i}\left(\lambda^{-1} a_2 - \frac{\lambda^{-2} a_1^2}{2}\right), \qquad b_3 = \frac{1}{2\pi i}\left(\lambda^{-1} a_3 - \lambda^{-2} a_1 a_2 + \frac{\lambda^{-3} a_1^3}{3}\right).$$

Hence the first component of BNF_m can be expressed in terms of the Birkhoff coefficients, b_i,

$$BNF_m(F) : (z,\bar{z}) \longmapsto R_{2\pi \frac{q}{m}}(e^{2\pi i \gamma(r)} z + c\bar{z}^{m-1}) + \mathcal{R}_{m+1}(z,\bar{z}), \tag{3.2}$$

where $\gamma(r) = \delta + b_1 r^2 + b_2 r^4 + \cdots + b_s r^{2s}, r = |z|$.

This is equivalent to write the first component of BNF_m as the composition

$$BNF_m(z,\bar{z}) = R_{2\pi q/m} \circ K(z,\bar{z},\delta),$$

where $K(z,\bar{z},\delta) = e^{2\pi i\gamma(r)}z + c\bar{z}^{m-1} + \hat{\mathcal{R}}_{m+1}(z,\bar{z})$ is a near-the-identity map such that the m-jet commutes with the rotation $R_{2\pi q/m}$. This commutativity, reveals that the reduction to BNF_m adds an extra symmetry. In particular, the dynamics of the m order resonance, can be analysed in terms of the near the identity map K.

3.2 Behaviour of α as a function of ε.

As shown in the previous section, the Birkhoff normal form of a one-parameter family of area preserving maps around an elliptic fixed point depends on the parameter δ. Also, the fixed points of an area preserving map have associated eigenvalues $\lambda = e^{\pm 2\pi i\alpha}$ that depend on this parameter since $\alpha = q/m + \delta$. In this section we want to see how the multiplier α depends on the original parameter ε of the Michelson system (1.1). For that, we will compute for some values of ε the fixed point of the Poincaré map and its eigenvalues.

Let $X : U \subset \mathbb{R}^3 \longrightarrow \mathbb{R}^3$ be a three dimensional vector field $\mathcal{C}^r, r \geqslant 1$, that we assume has a periodic orbit transverse to $\Sigma = \{g(x) = 0\}$. The Poincaré map $P : \Sigma \longrightarrow \Sigma$ is given by $x_1 = P(x_0) = \varphi(t_{x_0}, x_0)$, where $t_{x_0} = t(x_0)$ and $\varphi(t,x)$ is the flow associated to X.

The periodic orbit of the flow corresponds to a fixed point of the Poincaré map, so we use Newton's method to solve the system $P(x) - x = 0$. For that, we need to compute the derivative of the Poincaré map with respect to x_0,

$$\begin{aligned} DP(x_0) &= D_t\varphi(t_{x_0}, x_0)D_{x_0}(t_{x_0}) + D_{x_0}\varphi(t_{x_0}, x_0) \\ &= X(x_1)D_{x_0}(t_{x_0}) + D_{x_0}\varphi(t_{x_0}, x_0). \end{aligned}$$

To compute $D_{x_0}(t_{x_0})$ we differentiate the initial condition $g(x_1) = g(\varphi(t_{x_0}, x_0)) = 0$,

$$Dg(x_1)D\varphi(t_{x_0}, x_0) = Dg(x_1)DP(x_0) = 0.$$

This implies that

$$Dg(x_1)(X(x_1)D_{x_0}t_{x_0} + D_{x_0}\varphi(t_{x_0}, x_0)) = 0,$$

and thus

$$D_{x_0}(t_{x_0}) = \frac{-Dg(x_1)D_{x_0}\varphi(t_{x_0}, x_0)}{Dg(x_1)X(x_1)}.$$

Therefore,

$$DP(x_0) = -\frac{X(x_1)}{Dg(x_1)X(x_1)}[Dg(x_1)D_{x_0}\varphi(t_{x_0}, x_0)] + D_{x_0}\varphi(t_{x_0}, x_0).$$

We perform the corresponding computations for the Michelson system (1.1) considering the section $\Sigma = \{z = 0\}$. We have that $Dg(x_1, y_1, z_1) = (0, 0, 1)$ where $(x_1, y_1, z_1) =$

$P(x_0, y_0, z_0)$. Hence the differential of the Poincaré map is given by

$$DP(x_0, y_0, z_0) = -\frac{1}{\varepsilon(1-x_1^2)-y_1}\begin{pmatrix} y_1 \\ z_1 \\ \varepsilon(1-x_1^2)-y_1 \end{pmatrix}\begin{pmatrix} a_{31} & a_{32} & a_{33} \end{pmatrix} + \begin{pmatrix} a_{11} & a_{12} & a_{13} \\ a_{21} & a_{22} & a_{23} \\ a_{31} & a_{32} & a_{33} \end{pmatrix},$$

where $D_{x_0}\varphi(t_{x_0}, x_0) = (a_{ij})_{ij}$ is the first variational with respect to the initial condition. The matrix $D_{x_0}\varphi(t_{x_0}, x_0)$ is the solution of the variational equation

$$\frac{d}{dt}D_{x_0}\varphi(t_{x_0}, x_0) = DF(\varphi(t_{x_0}, x_0))D_{x_0}\varphi(t_{x_0}, x_0) = \begin{pmatrix} 0 & 1 & 0 \\ 0 & 0 & 1 \\ -2x_0\varepsilon & -1 & 0 \end{pmatrix} D_{x_0}\varphi(t_{x_0}, x_0),$$

with initial conditions $D_{x_0}\varphi(0, x_0) = Id$.
Thus we integrate with Taylor's method the equations of the system X together with the variational equations to find the image of the Poincaré map and we use the variational matrix to obtain the differential of P. This allows us to compute, for a given value of ε, the fixed point of P, which $y > 0$ and determine its multiplier $\alpha \in (0, 1)$ whenever it is elliptic. We denote λ and $1/\lambda$ the eigenvalues of DP at the fixed point.

On the left figure 3.1, we plot for each value ε between 0 and 0.4, the value of $\tilde{\alpha} = \arctan(Im(\lambda)/Re(\lambda))$ which coincides with the multiplier α of the fixed point if it is elliptic.

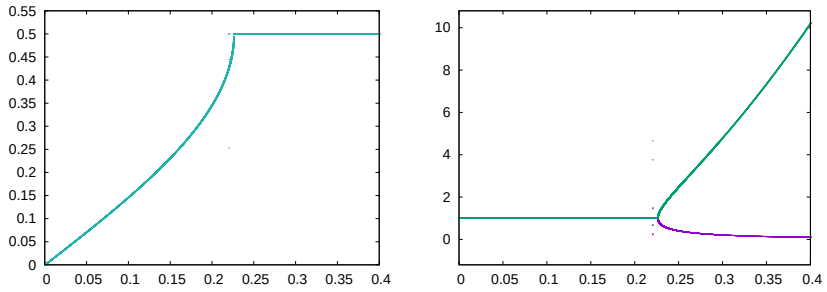

Figure 3.1: Left: We display $\tilde{\alpha}$ as a function of ε. Right: We display the modulus of λ and 1λ as a function of ε. We observe that the eigenvalues leave the unit sphere and becomes real for values of ε larger than $\varepsilon_* \approx 0.2258$.

Close to a resonant point, the Birkhoff normal form explained how the islands are generated, and we know that the value of δ depends on the sign of the first Birkhoff coefficient. For a given ε such that we have a resonance of order m, we will see m islands on the Poincaré section and that the corresponding α is equal to $q/m + \delta$. For $\varepsilon = 0.1405$, one can see in the plot that $\alpha \approx 0.214 = \frac{1}{5} + \delta$, so in the Poincaré section we see five islands. For $\varepsilon = 0.104$, one can see in the plot that $\alpha \approx 0.1527 = \frac{1}{7} + \delta$, so in the Poincaré section we see seven islands, see Figure 3.2.

In the following section, we will compute the first Birkhoff coefficient of the Birkhoff normal form for values of ε for which it has an elliptic fixed point.

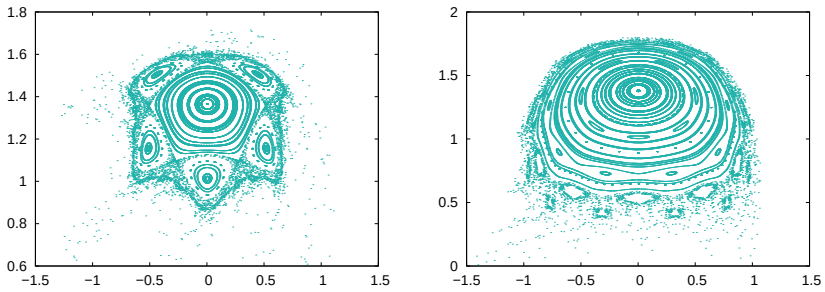

Figure 3.2: Poincaré section of the Michelson flow for $\varepsilon = 0.1405$ and 0.104.

At the right plot of Figure 3.1, we see the modulus of the eigenvalues for each value of the parameter. For a value $\varepsilon_* \approx 0.2258$ the eigenvalues of the fixed points are $\lambda = -1$ double, and we have a period-doubling bifurcation. The elliptic periodic orbit of the flow becomes a saddle and a new elliptic orbit with twice the period of the original appears. In the phase space of P we see that the invariant manifolds of the saddle orbit surround the new 2-periodic elliptic points and form almost a figure eight (the invariant manifolds are splitted, note that a small chaotic zone near the invariant manifolds is observed in Figure 3.3, left). Since the new 2-periodic orbit is elliptic, there are new KAM tori surrounding it. These tori form a Cantorian family, see related comments in section 3.5. Accordingly, we observe in Figure 3.3 left, invariant curves for P.

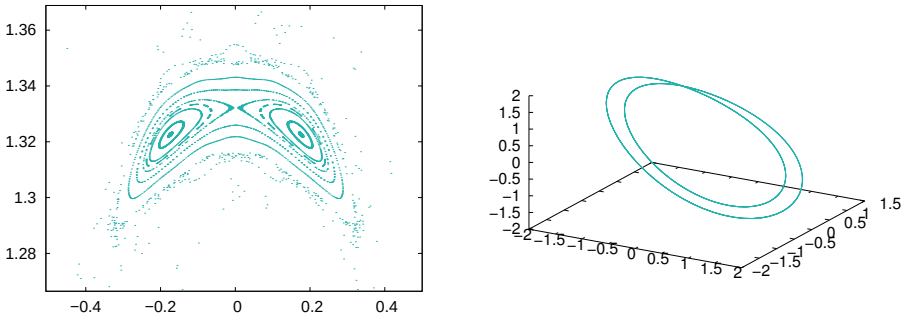

Figure 3.3: Left: Poincaré section of the Michelson flow for $\varepsilon = 0.228$, close to ε_*. One can observe the persistence of curves around the figure eight. Right: Elliptic periodic orbit of the flow for $\varepsilon = 0.228$.

Moreover the invariant curves far from the fixed point persist outside the eight figure after the bifurcation. This can be seen in Figure 3.3 left. Those tori outside the eight figure, define an stability domain which is bigger than the region bounded by the invariant manifolds of the hyperbolic point at $x = 0$. As ε grows, the region bounded by the invariant manifolds also grows and breaks these tori surrounding the figure eight.
For $\varepsilon = 0.228 > \varepsilon_*$ the two-periodic orbit of the Poincaré map corresponds to $x \approx 0.1751571$ and $y \approx 1.3225644$. We represent the elliptic periodic orbit of the flow in Figure 3.3 right.

3.3 Computing the first Birkhoff coefficient

To get a numerical approximation of the Birkhoff coefficients of the Michelson system, one has to reduce to Birkhoff normal form the Poincaré map. This is achieved by applying a sequence of changes of variable, as explained in section 3.1.

To compute the normal form, a Taylor expansion of the Poincaré map is needed. Since there is no explicit expression of the map, one can use jet transport method to get the jet of the Poincaré map. Indeed the coefficients of the Taylor expansion correspond (up to the factorials) to the derivatives of the Poincaré map, that can be computed with variational equations. This can be tough to write down explicitly and implement numerically for high orders, so we use jet transport to get these derivatives automatically.

As we have seen in section 2 one can construct a Poincaré section $\Sigma = \{g(x) = 0\}$ such that given an initial condition x_0, we get its image through the Poincaré map $P(x_0) = \varphi(t_{x_0}, x_0)$. To get the Taylor expansion of the Poincaré map we need to obtain $P(x_0 + \Delta x)$ for small variations Δx of the initial condition.
The main idea of the jet transport method is to integrate the ordinary differential equation replacing operations with numbers by operations with polynomials in Δx truncated up to some order n, [1]. This kind of algorithms can be also validated, see [18]. Since we use the internal PARI/GP polynomial arithmetics, [10], these replacement accounts for simple modifications of the code of the Taylor method used before, so that the computations are done considering polynomials in Δx. For more involved examples, one would require a proper implementation of the polynomial arithmetics, for example in C.

To compute the jet of the Poincaré map $P(x_0 + \Delta x) = \varphi(t_{x_0+\Delta x}, x_0 + \Delta x)$, we have to adjust the return time $t_{x_0+\Delta x}$ at each order imposing the condition at the Poincaré map $g(\varphi(t_{x_0+\Delta x}, x_0 + \Delta x)) = 0$. In the setting of the Michelson system, we consider $\Delta x = (dx, dy)$ and we deal with polynomials in two variables. Hence we look for a value $h = \sum_{i=1}^{n} \sum_{j=0}^{i} h_{ij} dx^i dy^j$ such that $g(\varphi(t_{x_0} + h, x_0)) = 0$, up to order n.
For that, we use Newton method to the function $g(\varphi(t_{x_0} + h, x_0))$ with an initial condition $h_{ij} = 0$. We compute the derivatives of g with respect to h_{ij} using that

$$D_{h_{ij}} g(\varphi(t_{x_0} + h, x_0)) = Dg(\varphi(t_{x_0} + h, x_0)) D_t \varphi(t_{x_0} + h, x_0) D_{h_{ij}} h.$$

Thus, we get the return time at each order and hence the jet of the Poincaré map for an initial condition $x_0 + \Delta x$.

When computing jet transport propagation, there is a numerical problem concerning the step size. In general there is no way to adjust properly the step size due to the fact that one has to use weighted norms with different weights at different orders of the polynomial. For computations we have just controled the step size according to the point x_0, ignoring the jet. However we have checked the computations choosing different maximum sizes of the step size, so that we can trust that at least enough number of digits are correct. In particular, we have chosen a maximum h of $10^{-1}, 10^{-2}$ and 10^{-3}, and the results obtained for the coefficients of the jet, coincide up to at least 10 digits in all cases. Computations where performed using multiprecision arithmetics with 38 digits, a Taylor method with order 50, and requiring a local error of 10^{-38} at each step of integration to determine the step size. The accuracy of the Newton method to compute the Poincaré map was 10^{-25}.

The Poincaré map can be expressed as

$$P(x,y) = \left(\sum_{r \geqslant 0} a_{kl} x^k y^l \ , \ \sum_{r \geqslant 0} b_{kl} x^k y^l \right),$$

where $r = k + l$. Using the previous jet transport algorithm for $\varepsilon = 0.15$, we obtain the coefficients a_{kl} and b_{kl} up to order three, that we show in the following table.

k	l	a_{kl}	b_{kl}
0	0	1.5022524073184e-30	1.4108703410470
1	0	0.9960522061745	0.0846779159768
0	1	-0.0930585322491	0.9960522061745
2	0	-0.0602100724979	-1.5496172357267e-5
1	1	-0.0002438305829	0.0597160872293
0	2	-0.0360883638716	-0.0043210072100
3	0	0.0036219356712	0.0016841575225
2	1	0.0014495161576	-0.0002592308733
1	2	-0.0002521608207	-0.0012129529626
0	3	-0.0012099020571	-0.0010831335070

In order to compute the Birkhoff normal form, we have to use complex coordinates and a linear change of variables to get the Poincaré map in the form

$$P(z,\bar{z}) = \left(\lambda z + \sum_{r \geqslant 2} \tilde{a}_{kl} z^k \bar{z}^l \ , \ \bar{\lambda} \bar{z} + \sum_{r \geqslant 2} \tilde{b}_{kl} z^k \bar{z}^l \right).$$

One can compute the determinant of the map up to order three to check that P does not preserves the canonical area form, as we proved in section 2. We get that

$$\det DP(z,\bar{z}) = 1 + dz + \bar{d}\bar{z} + \mathcal{O}(z\bar{z}),$$

where $d \approx 0.1007 + 0.0045i$, which is different from one, as we expected.

Once we have a Taylor expansion of the Poincaré map, we apply successively changes of variables to put the map in Birkhoff normal form up to some order, such that each change of variables $\phi^1_{X_{p+1}}$ attempt to remove the term of order p from the map. We remark that since the map is not canonical area preserving, we have not used canonical changes for the reduction in the implementations. We follow directly the scheme in [2]. But, since up to order three, these changes of variables are unique, the resulting Poincaré map truncated up to order three P_3, preserves the canonical area form, that is $\det DP_3(z,\bar{z}) = 1$.

Remark 3.4. For higher order reduction to normal form, the changes of variables would not be uniquely determined since the Poincaré map has resonant terms, so it will not necessarily preserve the standard area form.
However, the change of variables of the Darboux's theorem can be applied to get an area preserving Birkhoff normal form. Numerically, at each step that removes a term of order p, we would apply a change of variables such that the Birkhoff normal form up to order p preserves the standard form. We have not implemented such a higher order reduction.

Finally, once an approximation of the Birkhoff normal form (3.2) is computed, we get that the first Birkhoff coefficient for different values of ε are given in Figure 3.3.
To get high precision computations and use a polynomial arithmetic, the library PARI/GP has been used.

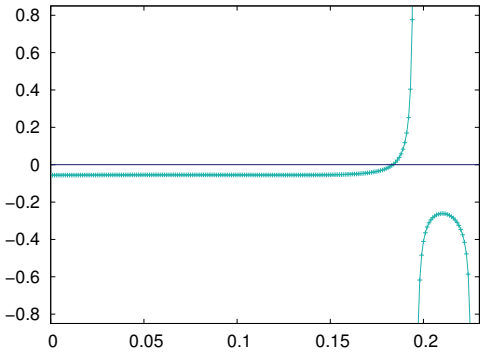

Figure 3.4: First Birkhoff coefficient of the Poincaré map of the Michelson system for values of ε between 0 and 0.2258.

As expected, the behaviour of the first Birkhoff coefficient with respect to ε shows some asymptotic. The first asymptotic that we can see in the plot corresponds to the value of ε for which there is a resonance of order 3. The second asymptotic occurs for $\varepsilon_* = 0.2258$ where we have a period-doubling bifurcation, and so the elliptic periodic orbit becomes a saddle.

Moreover, note that there is a value of ε for which $b_1 = 0$. This value corresponds to a point where the first order twist condition vanishes as we will explain in section 3.4.

3.4 Truncated Birkhoff normal form

Let us consider from now on the truncated Birkhoff normal form up to order m, (3.2). We will proof in this section that under certain conditions, the BNF_m has two periodic orbit of period m and how is the geometrical structure of the island. The first result is a consequence of the Poincare-Birkhoff theorem, [6]. Nevertheless here we will derive this result directly using a flow interpolation of the truncated Birkhoff normal form.

3.4.1 The interpolating Hamiltonian of BNF_m

Recall that the Birkhoff normal form up to order m is written as

$$BNF_m(z,\bar{z}) = R_{2\pi q/m} \circ K(z,\bar{z},\delta),$$

where $K(z,\bar{z},\delta) = e^{2\pi i\gamma(r)}z + c\bar{z}^{m-1} + \hat{\mathcal{R}}_{m+1}(z,\bar{z})$ is a near-the-identity map.

Note that scaling $z \longmapsto \mu z$ with a suitable complex μ in 3.2, we get a Birkhoff normal form expressed as $R_{2\pi(q/m)} \circ K(z,\bar{z},\delta)$ where

$$K(z,\bar{z},\delta) = e^{2\pi i\gamma(r)}z + i\bar{z}^{m-1} + R_{m+1}(z,\bar{z}).$$

The Birkhoff coefficients are modified according to $\tilde{b}_j = |\mu|^{2j} b_j$ that we will denote by b_j. Hence in the following we consider $c = i$.

In order to study the dynamics of a map close to the identity, it is useful to look for an autonomous vector field such that the time-1 flow associated gives a good approximation to the map, in a suitable neighbourhood of the m resonance. The existence of such a vector field follows from the suspension of the map after performing some steps of averaging to remove the dependence on t.

A suspension of a map F is non-autonomous periodic vector field f such that the associated Poincaré map coincides with the map. If F is a near-the-identity map that can be expressed as $F(x) = x + \varepsilon G(x)$ with ε sufficiently small, being G is a real analytic function, one can obtain f as a periodic non-autonomous vector field of period 1. The suspension can be given explicitly as a vector field $f(z,t) = \varepsilon\psi'(t)G(z)$ where ψ is an Hermite-like polynomial that interpolates $(0,0)$ and $(1,1)$ imposing null derivatives up to the desired order k. Thus $\psi(t) = t^k(2-t)^k$ and $\varphi_t(x) = x + \varepsilon\psi(t)G(x)$ is the time one flow such that the associated Poincaré map is F since $\varphi_0(x) = x$ and $\varphi_1(x) = F(x)$.

The suspension is a vector field of the form $\dot{z} = \varepsilon\tilde{f}(z,t)$ where $\tilde{f}$ is a time-periodic vector field [1]. Since t becomes a fast angle, one can perform a finite number of steps of averaging, and remove the dependence on t up to the desired order.

Since K is a near-the-identity map, we can compute a vector field such that the associated time-1 flow identity mapinterpolates K, see [36]. We include the details in the following.

Moreover, since K is symplectic, the vector field is Hamiltonian. A suitable autonomous vector field to describe the dynamics around the m order resonance is the following. Denote $\delta = b_0$ and define

$$\mathcal{H}_{nr}(I) = \pi \sum_{n=0}^{s} \frac{b_n}{n+1}(2I)^{n+1}, \qquad \text{and} \qquad \mathcal{H}_r(I,\varphi) = \frac{1}{m}(2I)^{\frac{m}{2}}\cos(m\varphi),$$

the non-resonant and resonant parts of the Hamiltonian, where (I,φ) are symplectic polar coordinates (also referred as Poincaré variables), defined by $z = \sqrt{2I}e^{i\varphi}$. Let r^* be such that $\gamma(r^*) = 0, r^* \approx (-\delta/b_1)^{1/2}$, where $b_1 \neq 0$.

Theorem 3.5. *Let $\hat{K}$ denote the original diffeomorphism K expressed in symplectic polar coordinates variables and assume $b_1 \neq 0$ and $m \geq 5$. Let $\nu > 0$ be a fixed value. Then the time-1 flow $\phi_{t=1}$ generated by the Hamiltonian*

$$\mathcal{H}(I,\varphi) = \mathcal{H}_{nr}(I) + \mathcal{H}_r(I,\varphi), \tag{3.3}$$

interpolates the map K with an error of order $m+1$ in the $(z,\bar{z})$-coordinates, that is,

$$\hat{K}(I,\varphi) = \phi_{t=1}(I,\varphi) + \mathcal{O}(I^{\frac{m+1}{2}}),$$

in an annulus centered in the resonance radius r_* of width $r_*^{1+\nu}$, for $|\delta|$ sufficiently small.

[1] Note that the suspension constructed above is analytic with respect to x but $\mathcal{C}^k$ in t. Taking k large enough, the required number of averaging steps over the fast frequency, can be performed

Proof. We consider the map $T(z,\bar{z}) = T_2 \circ T_1(z,\bar{z})$ where $T_1(z,\bar{z}) = e^{2\pi i\gamma(r)}z$ and $T_2(z,\bar{z}) = z + i\bar{z}^{m-1}$. One has

$$\begin{aligned} T(z,\bar{z}) = T_2 \circ T_1(z,\bar{z}) = T_2(e^{2\pi i\gamma(r)}z) &= e^{2\pi i\gamma(r)}z + i\left(e^{2\pi i\gamma(r)}\bar{z}\right)^{m-1} \\ &= e^{2\pi i\gamma(r)}z + i\bar{z}^{m-1}(1+\mathcal{O}(\delta)) = K(z,\bar{z}) + \mathcal{O}(r^{m+1}), \end{aligned}$$

for δ small enough. Hence K is order r^{m+1}-close to T.
Since T_1 is a rotation of angle $2\pi\gamma(r)$, in symplectic polar coordinates, it becomes $T_1(I,\varphi) = (I, \varphi + \omega(I))$ where $\omega(I) = 2\pi\gamma(I)$. That means that the flow $\dot{I} = 0, \dot{\varphi} = \omega(I)$ interpolates T_1 at integer times. In complex coordinates, this vector field is given by $\dot{z} = X_1(z,\bar{z}) = i\omega(I)z$. Below, we denote by ϕ_1^t the associated flow.

Moreover, T_2 is approximated up to order $\mathcal{O}(2m-3)$ by the time one map of the vector field $\dot{z} = X_2(z,\bar{z}) = i\bar{z}^{m-1}$. If ϕ_2^t is the flow of X_2,

$$\begin{aligned} \phi_2^t(z,\bar{z}) &= (z,\bar{z})^T + \frac{d}{dt}\phi_2^t(z,\bar{z})|_{t=1} + \frac{1}{2}\frac{d^2}{dt^2}\phi_2^t(z,\bar{z})|_{t=1} + \cdots \\ &= (z,\bar{z})^T + X_2(z,\bar{z}) + \frac{1}{2}DX_2(z,\bar{z})X_2(z,\bar{z}) + \cdots \end{aligned}$$

Then the first component of $\phi_2^1(z,\bar{z})$ is $z + i\bar{z}^{m-1} + \mathcal{O}(r^{2m-3})$.
Thus

$$K(z,\bar{z}) = T(z,\bar{z}) + \mathcal{O}(r^{m+1}) = T_1 \circ T_2(z,\bar{z}) + \mathcal{O}(r^{m+1}) = \phi_2^1(\phi_1^1(z,\bar{z})) + \mathcal{O}(r^{m+1}).$$

Finally we observe that

$$\phi_2^1(\phi_1^1(z,\bar{z})) - \phi_{1+2}^1(z,\bar{z}) = \frac{1}{2}\left(DX_2(z,\bar{z})X_1(z,\bar{z}) - DX_1(z,\bar{z})X_2(z,\bar{z})\right) + \cdots$$

where ϕ_{1+2}^t denotes the flow of the vector field $X_1 + X_2$. A simple check shows that the terms within the parenthesis are $\mathcal{O}(r^{m+1})$.
Therefore, the Lie bracket of both vector fields that interpolate T_1 and T_2 is a vector field of order higher than $m+1+\nu$ on the annulus of radius $r_*^{1+\nu}$ for $\nu > 0$, centered in the radius r_*. Changing coordinates and computing the Hamiltonian we get (3.3).

□

In what follows we will use this interpolation to prove some results on the phase space structure of the map F.

3.4.2 Birkhoff periodic orbits

If we assume that λ is not a root of unity for any order less of equal than m, the Birkhoff normal form (3.2) up to order m in symplectic polar coordinates (I,φ), where $z = \sqrt{2I}e^{i\varphi}$, is given by

$$BNF_m(F) : (I,\varphi) \longmapsto (I, \varphi + 2\pi\gamma(I))$$

where $\gamma(I) = \delta + b_1(2I) + b_2(2I)^2 + \cdots + b_s(2I)^{2s}$.

If $b_1 \neq 0$, one has $\gamma'(I) = 2b_1 + \cdots \neq 0$ and so the BNF restricted to an annulus $A = \{(I,\varphi) : I \in [a,b], \varphi \in [0,2\pi]\}$ is an integrable area preserving twist map $\forall a, b$, such that $b > a$.

Definition 3.6. An *area preserving twist map* is a integrable map of an annulus A such that $(I, \varphi) \longmapsto (I, \varphi + \alpha(I))$, and $\frac{d\alpha}{dI} = \alpha'(I) \neq 0$ for all $I \in [a, b]$.

Note that without the requirement that λ should not be equal to any root of unity, the Birkhoff normal form up to order m includes the resonant term $c\bar{z}^{m-1}$ and then the map is not integrable, it would be a perturbation of the integrable twist map

$$F_\varepsilon(I, \varphi) = (I + g(I, \varphi, \varepsilon), \varphi + \alpha(I) + f(I, \varphi, \varepsilon)),$$

where f and g are periodic functions of period 2π on φ.

The orbits of an integrable twist map are circles centered at the origin. The restriction of the integrable twist map to an invariant circle $I = I_0$, defines a map of S^1.

Definition 3.7. Let $f : S^1 \longrightarrow S^1$ be an homeomorphism of the circle and $\tilde{F} : \mathbb{R} \longrightarrow \mathbb{R}$ a lift of f. The *rotation number* of f is the limit

$$\alpha(\tilde{f}) := \lim_{n \longrightarrow \infty} \frac{\tilde{f}^n(x) - x}{n}.$$

Note that α exists for all $x \in \mathbb{R}$, is independent of x and well defined up to an integer. Moreover, the limit does not depend on the lift chosen, so $\alpha - \alpha(f) - \alpha(\tilde{f}(\mod 1))$ is well defined. An invariant circle such that $I = I_0$ has rotation number $\alpha(I_0)$.
If an invariant curve has a rational rotation number, every point of the curve is a periodic point. The Poincaré-Birkhoff theorem shows taht some of these periodic points survive for F_ε.

Theorem 3.8 (Poincaré-Birkhoff)**.** *Given any rational number, q/m, between $\alpha(a)/2\pi$ and $\alpha(b)/2\pi$, then there are $2m$ fixed points of $F_\varepsilon^m : (I, \varphi) \longmapsto (I_m, \varphi_m)$ satisfying*

$$(I_m, \varphi_m) = (I, \varphi + 2\pi q), \tag{3.4}$$

provided that $|\varepsilon|$ is sufficiently small.

A proof of this Theorem can be found in [6]. However we will use the Hamiltonian system from Theorem 3.5 to prove the existence of the points and its stability directly, as was done in [36].

In order to prove the existence of the periodic orbit, one can use the Birkhoff normal form expressed as a rotation composed with a near-the-identity map and this map can be interpolated by a time one flow of a Hamiltonian system $\mathcal{H} = \mathcal{H}_{nr} + \mathcal{H}_r$ where

$$\mathcal{H}_{nr}(I) = \pi \sum_{n=0}^{s} \frac{b_n}{n+1} (2I)^{n+1}, \qquad \text{and} \qquad \mathcal{H}_r(I, \varphi) = \frac{1}{m} (2I)^{\frac{m}{2}} \cos(m\varphi),$$

as we have seen in theorem 3.5.

Assume that $b_1 \neq 0$ and the coefficient of the resonant term of order m is non-zero. Given the Birkhoff normal form expressed as

$$R_{2\pi q/m} \circ K(z, \bar{z}, \delta),$$

where $K(z,\bar{z},\delta) = e^{2\pi i(\delta+b_1r^2+b_2r^4+\cdots+b_sr^{2s})}z + c\bar{z}^{m-1} + \hat{\mathcal{R}}_{m+1}(z,\bar{z})$, one can see that K has a fixed point if $r \approx (-\frac{\delta}{b_1})^{1/2}$. Then if $b_1\delta < 0$, K has a fixed point and then $R_{2\pi q/m} \circ K(z,\bar{z},\delta)$ has periodic orbits of period m. Therefore the dynamical system generated by F has a resonance of order m.
The following theorem will be stated as in [36], but in the proof we use the implicit function theorem to show the existence of the correction of I as a function of δ corresponding to the periodic points which was implicitly assumed in the reference.

Theorem 3.9. *For $b_1\delta < 0$, in the resonant zone of the BNF, there are two periodic orbits of period m located near two concentric circumferences and the closest orbit to the external one is elliptic while the nearest orbit to the internal circumference is hyperbolic.*

Proof. Suppose $b_1 > 0$ and $\delta < 0$ and the computations for $b_1 < 0$ and $\delta > 0$ are analogous. First we compute fixed points of the vector field generated by $\mathcal{H}(I,\varphi) = \mathcal{H}_{nr}(I) + \mathcal{H}_r(I,\varphi)$,

$$\frac{\partial \mathcal{H}}{\partial \varphi}(I,\varphi) = \frac{\partial \mathcal{H}_r}{\partial \varphi}(I,\varphi) = -(2I)^{\frac{m}{2}}\sin(m\varphi) = 0.$$

The non-trivial solution are given by $\sin(m\varphi) = 0$,

$$\varphi_j = \frac{j\pi}{m}, \qquad j = 0,\dots,2m-1.$$

To find a solution of $\frac{\partial \mathcal{H}}{\partial I} = 0$, we ignore the resonant terms to find an approximation I_* of the radius where the resonance of order m is located.
Ignoring the resonant terms from $\frac{\partial \mathcal{H}}{\partial I} = \frac{\partial \mathcal{H}_{nr}}{\partial I} + \frac{\partial \mathcal{H}_r}{\partial I} = \omega(I) + \frac{\partial \mathcal{H}_r}{\partial I} = 0$ we get that

$$\omega(I) = 2\pi\sum_{n=0}^{s} b_n(2I)^n = 2\pi\left(b_0 + 2b_1I + \cdots\right) = 0.$$

Hence a solution of this equation is

$$I_* = -\frac{\delta}{2b_1} + \mathcal{O}(\delta^2),$$

where $\delta = b_0$. Since $-\frac{\delta}{2b_1} > 0$, this value is an approximation of the radius where the resonances of order m are located, so we look for ΔI such that $I_* + \Delta I$ is a solution of $\frac{\partial \mathcal{H}}{\partial I}(I,\varphi_j)$, where $\varphi_j = \frac{j\pi}{m}, j = 0,\dots,2m-1$.

Given φ_j, we want to solve the equation $g(I) = \omega(I) + (-1)^{j+1}\frac{1}{2}(2I)^{m/2-1} = 0$. If $\Delta I_j = I - I_*$ then $g(I) = 0$ if and only if $\omega(\Delta I_j + I_*) + (-1)^{j+1}2^{m/2-2}(\Delta I_j + I_*)^{m/2-1} = 0$. Note that, since $\omega(I_*) = 0$, one has

$$\omega(\Delta I_j + I_*) = \omega(\Delta I_j + I_*) - \omega(I_*) = \Delta I_j\tilde{\omega}(\Delta I_j, I_*),$$

where $\tilde{\omega}(0,0) = \omega'(0) = 4\pi b_1 \neq 0$.
We consider the function $G : \mathbb{R}\times\mathbb{R} \longrightarrow \mathbb{R}$, given by

$$G(\Delta I_j,\nu) = \Delta I_j\tilde{\omega}(\Delta I_j,\nu) + (-1)^{j+1}2^{m/2-2}(\Delta I_j + \nu)(\Delta I_j + I_*)^{m/2-2}.$$

Since $m \geqslant 5$, G is a $\mathcal{C}^1$ function. We have that $G(0,0) = 0$ and $\frac{\partial G}{\partial \Delta I_j}(0,0) = \tilde{\omega}(0,0) \neq 0$. By the implicit function theorem there exists an open neighbourhood U of $\nu = 0$ and a function $\Delta I_j(\nu)$ such that $G(\Delta I_j(\nu), \nu) = 0$ for all $\nu \in U$. Chosen ΔI_j small enough, one can assure that $I_* \in U$, so that $G(\Delta I_j(I_*), I_*) = 0$, which is equivalent to $g(I_* + \Delta I_j(I_*)) = 0$. This shows the existence of the correction function.
Moreover, $\Delta I_j(\nu) = \Delta I_j(0) + (\Delta I_j)'(0)\nu + \mathcal{O}(\nu^2)$, with $\Delta I_j(0) = 0$ and

$$\begin{aligned}(\Delta I_j)'(0) &= -\left(\frac{\partial G}{\partial \Delta I_j}(0,0)\right)^{-1} \frac{\partial G}{\partial \nu}(0,0) \\ &= -(4\pi b_1)^{-1}\left((-1)^{j+1} 2^{m/2-2} I_*^{m/2-2}\right).\end{aligned}$$

Then $\Delta I_j(I_*) = \frac{(-1)^{j+1}(2I_*)^{\frac{m}{2}-1}}{4\pi b_1}(1 + \mathcal{O}(I_*))$.
Therefore the fixed points are $(\varphi_j, I) = \left(\frac{j\pi}{m}, I_* + \Delta I_j\right)$ for $j = 0, \ldots, 2m-1$. We compute the eigenvalues of the fixed points to get its stability,

$$\hat{\lambda}_j = \pm\left[(2I)^{\frac{m}{2}} m(-1)^j \left(\frac{\partial^2 \mathcal{H}_{nr}(I)}{\partial I^2} + \mathcal{O}((2I)^{\frac{m}{2}-2})\right)\right]^{\frac{1}{2}}, \qquad \frac{\partial^2 \mathcal{H}_{nr}(I)}{\partial I^2} = 4\pi b_1 + \mathcal{O}(\delta^\mu),$$

where $\mu = \min\{1, (m/2) - 2\}$.

Thus the fixed points such that j is even are hyperbolic, denoted as $H = (I_H, \varphi_H)$, while the ones with j odd are elliptic and denoted as $E = (I_E, \varphi_E)$.

From theorem 3.5 we have that the fixed points of $\mathcal{H}$ satisfy the condition $\hat{K}(I,\varphi) - (I,\varphi) = \phi_{t=1}(I,\varphi) + \mathcal{O}(I^{\frac{m+1+\nu}{2}}) - (I,\varphi) = 0$, where $\phi_{t=1}$ is the time one flow generated by $\mathcal{H}$. Bounding $\mathcal{O}(I^{\frac{m+1+\nu}{2}})$ by $\mathcal{O}(I^{\frac{m+1}{2}})$ one get

$$\phi_{t=1}(I,\varphi) - (I,\varphi) + \mathcal{O}(I^{\frac{m+1}{2}}) = 0.$$

Skipping the last term, the determinant of the differential of this equation at the fixed points is $-4\pi b_1 m (2I)^{\frac{m}{2}} \cos(m\varphi_j)(1 + \mathcal{O}(\delta)) \neq 0$. Then by the implicit function theorem $\hat{K}$ has the same number of periodic orbits located close to the ones of $\phi_{t=1}$. Note that, when taking into account the effect of the remainder, the corrections will depend on the concrete value of j. But they are small enough to be neglected.

□

3.4.3 Resonant islands

The invariant manifolds of the hyperbolic points H of the same resonance bound a chain of islands. The following theorem determines the width of an island in BNF_m coordinates, see [36].

Theorem 3.10. *Assume H and E are on the same island. Denote by p and q the points of the pendulum-like separatrices such that the distance from the circle of radius I_E reaches a maximum. Let δ_p and δ_q be these distances. Then the width of the resonance of order $m \geqslant 5$, $\delta_p + \delta_q$ is $\mathcal{O}(I_*^{\frac{m}{4}})$.*

Proof. Suppose $b_1 > 0$, the case for $b_1 < 0$ is analogous.
To look for the distances δ_p and δ_q up to first order, we use that p and q are on the separatrices and so $\mathcal{H}(H) = \mathcal{H}(p) = \mathcal{H}(q)$. We will do the computations for p and the argument can be repeated for the point q.

Given $H = I_* + \Delta I_H$ and $E = I_* + \Delta I_E$, we use the Taylor expansion of $\mathcal{H}$,

$$\mathcal{H}(H) = \mathcal{H}(I_* + \Delta I_H) = \mathcal{H}_{nr}(I_*) + \mathcal{H}_r(I_*, \varphi_H) + \left(\frac{\partial \mathcal{H}_{nr}}{\partial I}(I_*) + \frac{\partial \mathcal{H}_r}{\partial I}(I_*, \varphi_H)\right)\Delta I_H + \cdots$$
$$\mathcal{H}(E) = \mathcal{H}(I_* + \Delta I_E) = \mathcal{H}_{nr}(I_*) + \mathcal{H}_r(I_*, \varphi_E) + \left(\frac{\partial \mathcal{H}_{nr}}{\partial I}(I_*) + \frac{\partial \mathcal{H}_r}{\partial I}(I_*, \varphi_E)\right)\Delta I_E + \cdots$$

For $p = E + \delta_p$, we get

$$\mathcal{H}(p) = \mathcal{H}(E) + \frac{\partial \mathcal{H}}{\partial I}(E)\delta_p + \frac{1}{2}\frac{\partial^2 \mathcal{H}}{\partial I^2}(E)\delta_p^2 + \cdots$$

Imposing that $\mathcal{H}(H) = \mathcal{H}(p)$, the non-resonant terms are cancelled and we have that

$$\begin{aligned}&\mathcal{H}_r(I_*, \varphi_H) + \left(\frac{\partial \mathcal{H}_{nr}}{\partial I}(I_*) + \frac{\partial \mathcal{H}_r}{\partial I}(I_*, \varphi_H)\right)\Delta I_H + \cdots \\ &= \mathcal{H}_r(I_*, \varphi_E) + \left(\frac{\partial \mathcal{H}_{nr}}{\partial I}(I_*) + \frac{\partial \mathcal{H}_r}{\partial I}(I_*, \varphi_E)\right)\Delta I_E + \frac{\partial \mathcal{H}}{\partial I}(E)\delta_p + \frac{1}{2}\frac{\partial^2 \mathcal{H}}{\partial I^2}(E)\delta_p^2 + \mathcal{O}(\delta_p^3).\end{aligned}$$

We compute the terms of this equality to get an approximation of δ_p.

Since $I = I_*$ is a curve of fixed points of the Hamiltonian $\mathcal{H}_{nr}$, $\frac{\partial \mathcal{H}_{nr}}{\partial I}(I_*) = 0$. As E is a fixed point of $\mathcal{H}$, $\frac{\partial \mathcal{H}}{\partial I}(E) = 0$.
Moreover $\mathcal{H}_r(I_*, \varphi_H) = -\mathcal{H}_r(I_*, \varphi_E) = \frac{1}{m}(2I_*)^{\frac{m}{2}}$, and thus

$$\frac{\partial \mathcal{H}_r}{\partial I}(I_*, \varphi_H) = -\frac{\partial \mathcal{H}_r}{\partial I}(I_*, \varphi_E) = (2I_*)^{\frac{m}{2}-1},$$

Finally, $\Delta I_H = -\Delta I_E + \mathcal{O}(I_*^{\frac{m}{2}})$, and $\frac{\partial^2 \mathcal{H}}{\partial I^2}(E) = 4\pi b_1 + \mathcal{O}(I_*^{\mu})$ where $\mu = \min\{1, \frac{m}{2} - 2\}$.
Therefore $\mathcal{H}(H) = \mathcal{H}(p)$ is equivalent to

$$\frac{2}{m}(2I_*)^{\frac{m}{2}} + 2(2I_*)^{\frac{m}{2}-1}\Delta I_H = 2\pi b_1 \delta_p^2 + \mathcal{O}(I_*^{\mu}\delta_p^2, \delta_p^3).$$

Since ΔI_H is the correction of the fixed point, it is of order $I_*^{\frac{m}{2}-1}$ and so the term $2(2I_*)^{\frac{m}{2}-1}\Delta I_H$ is of order $\mathcal{O}(I_*^{m-2})$. Therefore

$$\frac{2}{m}(2I_*)^{\frac{m}{2}} = 2\pi b_1 \delta_p^2 + \mathcal{O}(I_*^{m-2}, I_*^{\mu}\delta_p^2, \delta_p^3).$$

From this equality,

$$\delta_p = \left(\frac{(2I_*)^{m/2}}{m\pi b_1}\right)^{1/2}(1 + \mathcal{O}(I_*^{\mu})).$$

Doing analogous computations, we get that $\delta_q = \mathcal{O}(I_*^{m/4})$ and then the width of the resonance of order $m \geqslant 5$, $\delta_p + \delta_q$ is $\mathcal{O}(I_*^{m/4})$. □

This theorem explains the growth of the resonant islands when they leave a neighbourhood of the origin. Nevertheless, we remark that this result is local, in particular it is only valid in the domain where BNF_m gives a good approximantion of F. Moreover it ignores the presence of other resonances in phase space.

The phase space of the Birkhoff normal form just contains the invariant curves and the island of period m. However we are interested on the dynamics of the two-dimensional map F, which in a neighbourhood of a fixed point can be seen as a perturbation of the BNF. Clearly the island structure remains similar, because hyperbolic points are persistent, but the unstable and stable invariant manifolds of the hyperbolic points generically will not coincide (and in the analytic case, have an exponentially small splitting in the perturbation parameter). In the next section we are going to study the persistence of invariant tori.

3.5 Persistence of invariant objects

As we have seen in the previous section, the Birkhoff normal form of an area preserving map can be expressed as a perturbation of an integrable twist map

$$F_\varepsilon(I,\varphi) = (I + g(\varphi, I, \varepsilon), \varphi + \alpha(I) + f(\varphi, I, \varepsilon)),$$

where f and g are periodic functions of period 2π on φ. By hypothesis, any twist map has invariant curves, so we want to see if they persist for F_ε. Hence this section is devoted to ensure the existence of invariant curves for area preserving maps, which is given by Moser Twist theorem, see either [6] or [34].

Theorem 3.11 (Moser Twist)**.** *Consider the map given by*

$$F_\varepsilon(I,\varphi) = (I + g(\varphi, I, \varepsilon), \varphi + \alpha(I) + f(\varphi, I, \varepsilon),$$

defined in the annulus $|I - I_0| < \rho$, where I, φ are real variables, f, g and α are real analytic functions and, f and g are periodic in φ with period 2π.

Assume also that F_ε satisfies the following conditions:

1. *F_ε is an area preserving map and α satisfies $\frac{d\alpha}{dI} \neq 0$.*
2. *Any closed curve $I = l(\varphi) = l(\varphi + 2\pi)$ near a circle and lying in the annulus intersects its image $F_\varepsilon(l)$.*
3. *Let I^* belong to the annulus and be such that $\omega = \alpha(I^*)$ satisfies*

$$\left| \frac{\omega}{2\pi} - \frac{p}{q} \right| \geqslant \frac{\gamma}{|q|^\tau},$$

for some $\omega > 0$, $\tau > 2$ and all integers $p, q \neq 0$.

Then if ε is sufficiently small,

(a) There exists a closed invariant curve

$$\Gamma(\varphi, I) = (\varphi + G(\varphi, \varepsilon), F(\varphi, \varepsilon)),$$

with $0 \leqslant \varphi \leqslant 2\pi$, such that F and G are real analytic, periodic with period 2π and tend to zero if $\varepsilon \longrightarrow 0$.

(b) The map F_ε on Γ is a rotation with rotation number ω and is given by $\varphi \longmapsto \varphi + \omega$.

Although we do not include the proof of this theorem, we want to comment on several aspects of it, so that the conditions required in the theorem can be properly understood.

1. Note that the conditions 1 and 3 of the theorem are satisfy for many values, so there exists many invariant curves on the annulus for a small value of ε. The third condition is called the Diophantine condition and deals with the problem of how the rotation number ω is approximated by rational numbers. In particular, it can be shown that the subset of ω values for which condition 3 does not hold has measure zero, see [5].

2. To see the existence of the invariant curve Γ, one strategy is to use an infinite sequence of changes of coordinates such that at each step, the new map is closer to a twist map. That means that we apply successively changes of coordinates U_i such that the new map F_i is closer to a twist map, and satisfies $U_i F_i = F_\varepsilon U_i$. This equality yields to a system of differential equations, that has a solution if ω satisfies the Diophantine condition. This is called the problem of small divisors.

3. It is proved that the Fourier series converge despite the presence of small divisors, [6].

4. The twist condition is needed to assure that the homological equation has zero mean and the requirement that ε is small is needed to make the sequence of changes of variables convergent for a diophantine frequency.

This theorem allow us to prove the existence of invariant curves for the Poincaré map. That means that the corresponding invariant tori of the original three dimensional volume preserving flow also persist.

An alternative approach to prove the persistence of the tori for the flow could be to apply KAM theory for three dimensional conservative flows. Although we postpone to future works the detailed study of KAM theory for three dimensional flows, we mention two possible strategies.

Note that in a neighbourhood of an elliptic periodic orbit, the flow has two angles and one action, hence the frequency map is not one-to-one. This means that the frequencies of an specific tori cannot be maintained when perturbing. The standard KAM techniques can be adapted to this setting by adding extra parameters. We refer to [11] for further details. Here we just want to mention that with these ideas the persistence of a Cantor set of tori can be proved.

Another way to prove the persistence of the KAM tori in this setting could be to apply the ideas of [12]. Although in the reference the theorem is stated by diffeomorphism, it seems to hold with minor modifications for limiting flows of a family of near-the-identity maps. This result gives the existence of invariant tori in a small neighbourhood of the elliptic curve.

Chapter 4

Invariant manifolds and their splitting

In this chapter we compute the invariant manifolds of the Michelson system. The illustrations below show that the one dimensional invariant manifolds do not intersect while the two dimensional ones intersect transversely along heteroclinic orbits. We present some available results describing the asymptotic behaviour of such splittings.

4.1 Invariant manifolds

As we have seen in section 1.2, the stable and unstable invariant manifolds of the saddle-focus fixed points $x_\pm$ are such that $\dim W^u(x_+) = \dim W^s(x_-) = 2$ and $\dim W^s(x_+) = \dim W^u(x_-) = 1$. It is important to study the intersection of the invariant manifolds and their splitting. Transversal intersections create chaos and the splitting size is related to the size of the chaotic zone created.

To get a numerical approximation of the invariant manifolds of the system, we will use a linear approximation of the manifolds using the corresponding eigenvectors. Recall that the fixed points $x_\pm = (\pm 1, 0, 0)$ have eigenvalues $\lambda \in \mathbb{R}$ and $\mu^\pm_{x_\pm} = \frac{-\lambda_{x_\pm} \pm i\sqrt{3\lambda^2_{x_\pm}+4}}{2} \in \mathbb{C}$. Then the eigenvectors are $v_{\lambda_{x_\pm}} = (1, \lambda_{x_\pm}, \lambda^2_{x_\pm})$ and $v_{\mu^\pm_{x_\pm}} = (1, \mu^\pm_{x_\pm}, {\mu^\pm_{x_\pm}}^2)$ respectively.

For the one-dimensional manifold, we simply integrate an initial point chosen closed enough to the fixed point in the direction of the eigenvector $v_{\lambda_{x_\pm}}$. For the two-dimensional, we consider a set of initial conditions $x_\pm + \delta v$ where $v \in \langle \mu^+_{x_\pm}, \mu^-_{x_\pm} \rangle$ and δ is the distance to the fixed point that we choose accordingly to have the desired accuracy in the linear approximation. For illustrations, we choose $n = 123$ points at a distance δ.
The propagation of the initial conditions is performed using the Taylor method to integrate the flow. In Figure 4.1 one can see the one-dimensional and two-dimensional manifolds of the fixed points $x_\pm$ for $\varepsilon = 0.01$.

As we have seen in section1.2, for small values of ε the manifolds nearly coincide and the two-dimensional manifolds delimits a set of two-dimensional tori which resembles the

bubble of stability of the limit system.

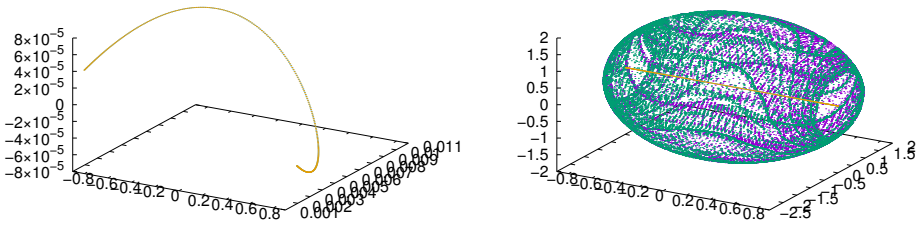

Figure 4.1: Invariant manifolds of the Michelson system for $\varepsilon = 0.01$.

For all $\varepsilon > 0$, see for example Figure 4.2, the manifolds do not coincide. In particular, the one-dimensional manifolds rotates one around the other one. This creates a channel through which point can travel from a neighbourhood of x_- to x_+. By the λ-Lemma, see [32, 6], the three-dimensional loops originated by the splitting of the two-dimensional invariant manifolds accumulate towards the one-dimensional invariant manifold, and peaces of the two-dimensional stable and unstable manifolds are contained in the channel and are responsible of the chaos inside. This is illustrated in Figure 4.5, where the intersections of the two-dimensional invariant manifolds with a suitable sections is shown.

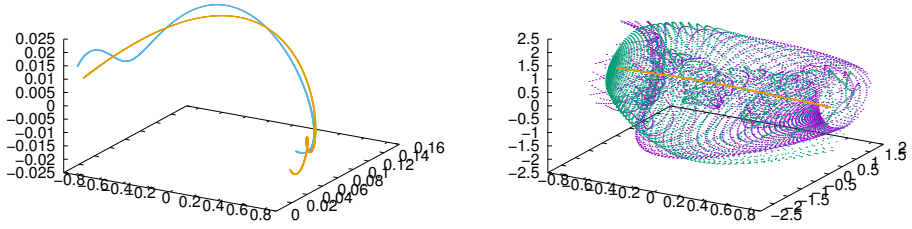

Figure 4.2: Invariant manifolds of the Michelson system for $\varepsilon = 0.15$.

The two-dimensional invariant manifolds intersect transversely, so that we can compute the splitting of the manifolds in a suitable section for some values of the parameter ε, as we will see in section 4.2.

In particular, in Figure 4.3 one can see the intersection of both one-dimensional and two-dimensional invariant manifolds with the Poincaré section $\Sigma = \{z = 0\}$, for values of $\varepsilon = 0.1$ and 0.15.

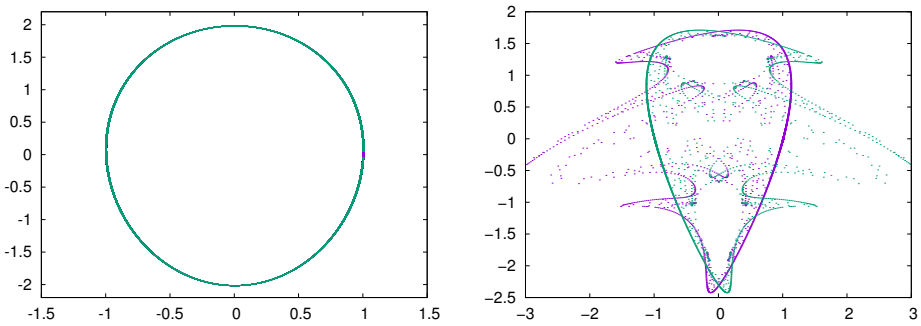

Figure 4.3: Intersection of the invariant manifolds with the Poincaré section $\Sigma = \{z = 0\}$ for $\varepsilon = 0.1$ and 0.15.

4.2 Assymptotic behaviour of the splitting

As pointed out before, the main features of the phase space of the Michelson system are consequences of the fact that it is a perturbation of a system having a bubble of stability. For three-dimensional flow, such a bubble structure is, generically, created at a Hopf-zero bifurcation. This bifurcation describes how a point bifurcates into a pair of saddle-foci that, for suitable parameters of the unfolding, their unstable and stable two-dimensional manifolds form an invariant ellipsoid, that is the bubble. At the bifurcation instant, the fixed point (the HZ singularity) has a zero eigenvalue and a pair of simple purely imaginary eigenvalues.

One tries to investigate the possible dynamics near an HZ singularity. To this end, the system is embedded into a two-parameter arbitrary family of systems (with divergence zero, in the conservative case). The formal series expansion of an arbitrary system of the family is simplified by reducing the system to normal form. One can see, [19], that generic unfolding of HZ singularities of codimension two can be written, at the 2-jet level as

$$\begin{aligned} x' &= -y + \mu x - axz, \\ y' &= x + \mu y - ayz, \\ z' &= \lambda + z^2 + b(x^2 + y^2). \end{aligned} \tag{4.1}$$

Here λ, μ are the parameters of the family. The previous unfolding preserves volume if $\mu = 0$ and $a = 1$. In this case, the Hopf-zero bifurcation is of codimension one.
When $\mu = 0$, the unfolding has a rotational symmetry and the two-dimensional unstable and stable invariant manifolds of the saddle-foci coincide. Taking cylindrical coordinates $r = \sqrt{x^2 + y^2}$, when $\mu = 0$, the function

$$H(r, z) = r^{2/a}\left(\lambda + z^2 + \frac{b}{1+a}r^2\right),$$

becomes a fist integral of the family.

The integrable structure can be destroyed under the effect of higher order terms. Under generic conditions, one can prove that there exists a bifurcation curve in the two-parameter phase space, where system shows again an invariant ellipsoid formed by the

two-dimensional invariant manifold of the equilibrium points at the vertical axis, see [20]. Generically, the 2d invariant manifolds will intersect transversely and the two-dimensional connection between the one-dimensional invariant manifolds will break. The splitting of the invariant manifolds makes homoclinic orbits possible.

We shall describe the asymptotic behaviour of both splittings. To this end, we need to introduce suitable splitting functions. For concreteness, we will focus on the Michelson system, that corresponds to an unfolding of the HZ singularity (4.1) with values $a = 1$ and $b = 1/2$, as was pointed out in [8].

To study the splitting functions of the Michelson system (1.1), we scale the variables $X = -x, Y = -\varepsilon^{-1/3}y, Z = -\varepsilon^{-2/3}z, \tau = \varepsilon^{1/3}t$, so that it can be expressed as

$$\begin{aligned}
\dot{X} &= -\dot{x}\frac{dt}{d\tau} = y\varepsilon^{-1/3} = Y,\\
\dot{Y} &= -\varepsilon^{-1/3}\dot{y}\frac{dt}{d\tau} = -\varepsilon^{-1/3}z\varepsilon^{-1/3} = Z,\\
\dot{Z} &= -\varepsilon^{-2/3}\dot{z}\frac{dt}{d\tau} = -\varepsilon^{-2/3}(\varepsilon(1-x^2)-y)\varepsilon^{-1/3} = -(1-x^2)+\varepsilon^{-1}y = -1+X^2+\alpha Y.
\end{aligned} \tag{4.2}$$

where $\alpha = -\varepsilon^{-2/3} > 0$.
As we have seen in section 1.1, it has a Hopf-zero bifurcation when $\varepsilon \longrightarrow 0$, or equivalently when $\alpha \longrightarrow -\infty$. Given the fixed points $X_\pm = (\pm 1, 0, 0)$ we want to study the behaviour of the splitting of the one-dimensional and two-dimensional invariant manifolds when $\alpha \longrightarrow -\infty$, [15].

Since the Michelson system is reversible for $R(X, Y, Z) = (-X, Y, -Z)$, we can do computations for invariant manifolds of X_- and use reversibility to find the equivalent for X_+.

To measure the splitting of the one-dimensional manifolds, one can measure the distance between the first intersection of $W^u(X_-)$ with $X = 0$ and $W^s(X_+)$ with $X = 0$. Indeed, by reversibility, if the first intersection of $W^s(X_+)$ with $X = 0$ occurs at $(Y^*(\alpha), Z^*(\alpha))$ then the first intersection of $W^u(X_-)$ with $X = 0$ occurs at $(Y^*(\alpha), -Z^*(\alpha))$. Then one can measure the splitting in the Z direction and it can be given as $S^{(1)}(\alpha) = 2\|Z^*(\alpha)\|$.

The asymptotic behaviour of the splitting of the one-dimensional manifolds of the Michelson system was given in [33]. The authors consider the equation

$$\delta w''' + w' = 1 - w^2, \qquad ' = \frac{d}{ds},$$

which is equivalent to the Michelson system (4.2) for $w = X, w' = -\alpha Y$ and $w'' = -\alpha^2 Z$, and reescaling the time by $s = \alpha^{-1}\tau$ where $\alpha = -\delta^{-1/3}$, and prove the following theorem.

Theorem 4.1. *For the unique solution $w(t)$ satisfying $w(0) = 0$, $w'(0) > 0$ on $[0, \infty]$ and $w(\infty) = 1$, we have*

$$w''(0) \sim A\delta^{-2}\exp\left(\frac{-\pi}{2\sqrt{\delta}}\right),$$

as $\delta \longrightarrow 0^+$ for some positive constant A.

Since $Z = -\alpha^2 w''$, this theorem gives an approximation of $Z^*(\delta)$, which is the Z coordinate of the intersection point of $W^u(X_+)$ with $X = 0$. Hence the splitting function is given by

$$\tilde{S}^{(1)}(\delta) = 2\|Z^*(\delta)\| = 2A\delta^{-2}\exp\left(\frac{-\pi}{2\sqrt{\delta}}\right) + o\left(\frac{-\pi}{2\sqrt{\delta}}\right).$$

Taking into account that $\delta^{-1/3} = |\alpha| = \varepsilon^{-2/3}$, the splitting function between the one-dimensional invariant manifolds of the system (1.1) is $S^{(1)}(\varepsilon) = \varepsilon^{-2}\tilde{S}^{(1)}(\varepsilon^2)$, which is given by

$$S^{(1)}(\varepsilon) = C\varepsilon^{-2}\exp\left(-\frac{\pi}{2\varepsilon}\right) + o\left(\exp\left(-\frac{\pi}{2\varepsilon}\right)\right), \tag{4.3}$$

for some positive constant C.

Numerically we can check this behaviour by computing for different values of ε, the intersection between the one dimensional invariant manifold $W^u(x_-)$ and $x = 0$. Due to reversibility of the system, the splitting function is given by $S^{(1)}(\varepsilon) = 2\|z^*(\varepsilon)\|$ where $z^*(\varepsilon)$ is the z coordinate of the intersection. In Figure 4.4, the logarithm of the splitting $S^{(1)}(\varepsilon)$ is shown as a function of ε.

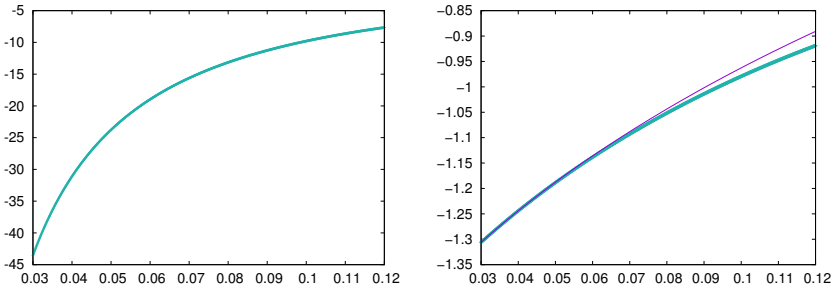

Figure 4.4: Left: Logarithm of the splitting $S^{(1)}(\varepsilon)$ as a function of ε, for $\varepsilon \in [0.03, 0.12]$. Right:

If $S^{(1)}$ depends on ε as $a\varepsilon^b \exp\left(-\frac{\pi}{2\varepsilon}\right)$, we have that

$$\varepsilon \log(S^{(1)}) \sim a\varepsilon + b\varepsilon\log(\varepsilon) - \pi/2,$$

and we can look for a function $f(x) = ax + bx\log(x) + c$ that fits $\varepsilon\log(S^{(1)})$. Performing the fitting for $\varepsilon \in [0.03, 0.04]$ we obtain $b = -2.52612$ and $c = -1.57942$. Moreover, imposing that $c = -\pi/2$, we get that $b \approx -2.27875$. The results are compatible with the splitting function 4.3. In Figure 4.4 right, we represent both εS^1 and the fitting function.

Moreover, in [15] it was observed that for all $\varepsilon > 0$ there is no solution with $x(t)$ monotone and connecting the equilibrium points along the one dimensional invariant manifolds. As a consequence

$$S^{(1)}(\varepsilon) \neq 0 \text{ for all } \varepsilon > 0, \tag{4.4}$$

that is, the one-dimensional invariant manifolds never coincide. This is shown in Figure 4.2 where we see that one manifold rotates around the other one.

To measure the splitting of the two-dimensional manifolds, one can introduce a suitable splitting function $S^{(2)}$. The section $X = 0$ is not transverse to the flow along $W^u(X_+)$, but in [15] a suitable section was introduced such that it first intersection with $W^u(X_+)$ is a closed curve. The section for the system 4.2 is given by $\Sigma_{\tilde{g}} = \{(X, Y, Z) \in \mathbb{R}^3 : \tilde{g}(X, Y, Z) = 0\}$ where

$$\tilde{g}(X, Y, Z) = |\alpha|^4 X + (|\alpha|^3 - 2)Z + (|\alpha|Y - 1)(2|\alpha|X + 3Z/2).$$

Using coordinates x, y and z of the system (1.1), this section correspond to $\Sigma_g = \{(x, y, z) \in \mathbb{R}^3 : g(x, y, z) = 0\}$ where

$$g(x, y, z) = x + (1 - 2\varepsilon^2)z - \varepsilon(y + \varepsilon)(2x + 3/2z).$$

Clearly this function respect the symmetry $(x, y, z) \longmapsto (-x, y, -z)$.

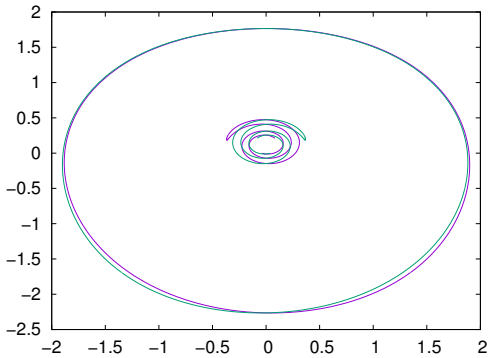

Figure 4.5: First and second intersections of $W^u(x_+)$ and $W^s(x_-)$ with Σ_g for $\varepsilon = 0.12$.

The intersections of $W^u(x_+)$ and $W^s(x_-)$ with Σ_g give two closed curves that are topologically S^1. These intersections are shown in Figure 4.5. To measure the splitting, one considers radial coordinates (r, φ) in Σ_g and, for each angle φ, the distance in r is measured. This gives a function $S^{(2)}(\varphi, \varepsilon)$, which measures the absolute value of the difference of the corresponding radii of the intersection of W^u and W^s with Σ_g.

For the Michelson system, in [8] it was shown that the splitting function is bounded by

$$S^{(2)}(\varphi, \varepsilon) \leqslant C\varepsilon^{-4} \exp\left(-\frac{\pi}{2\varepsilon}\right),$$

for some positive constant C. The exponential part and the power of the prefactor of the previous upper bound also hold for the asymptotic behaviour of the splitting as a function of ε, but the constant C should be replaced by a bounded function depending on ε.

We see in Figure 4.5 that the invariant manifolds intersect in two points, located in $x = 0$, one in $y \approx 1.76$ and the other one in $y \approx -2.64$, for $\varepsilon = 0.12$. The fact that there exists

exactly two heteroclinic connections for ε small was observed in [15].

For any map of the family of the unfolding of the HZ singularity (4.1) with $a > 0$ and $b > 0$, which are the cases for which the unfolding has a bubble structure, the same splitting functions are introduced and similar upper bounds can be obtained. Concretely, in [8] the authors prove

$$S^{(1)} \leqslant C_1 \varepsilon^{-(1+a)} \exp\left(-\frac{\pi}{2\varepsilon}\right); \qquad S^{(2)} \leqslant C_2 \varepsilon^{-2-\frac{2}{a}} \exp\left(-\frac{\pi}{2a\varepsilon}\right),$$

for some constants $C_1, C_2 > 0$.

Chapter 5

The Michelson map

In this chapter, we would like to comment on some aspects of the dynamics of a conservative three dimensional flow under a periodic forcing. This type of systems can be reduced to three dimensional volume preserving maps. To be able to perform some computations to illustrate the dynamics of these kind of maps, we will focus in the study of a discretization of the Michelson system.

The Michelson map that we consider is obtained as follows. Performing one step of the Euler method with step size $\varphi > 0$ to integrate the Michelson flow we get

$$\begin{cases} \overline{u} = u + \varphi v \\ \overline{v} = v + \varphi w \\ \overline{w} = w + \varphi(\varepsilon(1-u^2) - v) \end{cases}$$

with $\varepsilon \geqslant 0$. This map does not preserve volume so we slightly modify it. The map $\bar{x} = M_{\varepsilon,\varphi}(x)$ that we are going to use is

$$\begin{cases} \overline{u} = u + \varphi v \\ \overline{v} = v + \varphi \overline{w} \\ \overline{w} = w + \varphi(\varepsilon(1-u^2) - v) \end{cases} \tag{5.1}$$

This map was introduced in [27], but several questions about its dynamics remain open. This system is clearly volume preserving since

$$\det DM_{\varepsilon,\varphi} = \begin{pmatrix} 1 & \varphi & 0 \\ -2u\varepsilon\varphi^2 & 1-\varphi^2 & \varphi \\ -2u\varepsilon\varphi & -\varphi & 1 \end{pmatrix} = 1 - \varphi^2 - 2u\varepsilon^2\varphi^2 + \varphi^2 + 2u\varepsilon^2\varphi^2 = 1.$$

The map $M_{\varepsilon,\varphi}$ has fixed points $p_\pm = (\pm 1, 0, 0)$. To study the stability of these points with respect to the parameter ε and φ, one consider the linearised system at $p_\pm$ and study the eigenvalues of

$$DM_{\varepsilon,\varphi}(p_\pm) = \begin{pmatrix} 1 & \varphi & 0 \\ \mp 2\varepsilon\varphi^2 & 1-\varphi^2 & \varphi \\ \mp 2\varepsilon\varphi & -\varphi & 1 \end{pmatrix}.$$

Thus the eigenvalues are solutions of the equation $P(\lambda) = \lambda^3 + (\varphi^2 - 3)\lambda^2 + (\pm 2\varepsilon\varphi^3 - \varphi^2 + 3)\lambda - 1 = 0$.

We have computed those eigenvalues numerically, for different values of ε and φ, both between 0 and 1. We get that both fixed points has a real eigenvalue $\lambda_{p_\pm}$, and two complex conjugated $\mu^{\pm}_{p_\pm}$. One can see in Figure 5.1 how the eigenvalues depend on the parameters ε and φ. As we can see, in both cases when φ tends to zero, the eigenvalues have a linear behaviour. Therefore, we can assure for $\varepsilon \in [0,1]$ and $\varphi \in [0,1]$ that both fixed points $p_\pm$

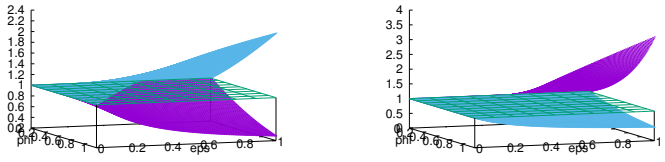

Figure 5.1: Left:Real eigenvalues $\lambda_{p_\pm}$. Right: Modulus of the eigenvalues $\mu^{\pm}_{p_\pm}$. In both plots, the eigenvalues of p_+ are shown in purple and the ones of p_- in blue.

are of saddle-focus type and they have the unstable and stable invariant manifolds such that $\dim W^s(p_+) = \dim W^u(p_-) = 1$ and $\dim W^u(p_+) = \dim W^s(p_-) = 2$.

As for the Michelson flow, we will show numerically, that the two-dimensional invariant manifolds of the map do not coincide, and that their intersections provide a continuum of heteroclinic orbits of the map.

We note that the Michelson system does not admit any smooth reversibility. We recall that a map F is reversible if it is conjugate to its inverse by an involution R, that is, if there exists R such that $R \circ F = F^{-1} \circ R$, $R^2 = Id$.

Theorem 5.1. *The Michelson map $M_{\varepsilon,\varphi}$ does not admit any smooth reversibility R.*

Proof. $M_{\varepsilon,\varphi}$ is a quadratic volume-preserving map of $\mathbb{R}^3$. By denoting $X = (x,y,z)$, $b = M_{\varepsilon,\varphi}(0)$, $A = DM_{\varepsilon,\varphi}(0)$, $v = (0,0,1)^T$, and $P = -2\varphi\epsilon e_1 e_1^T$, where e_i is the i-th vector of the canonical basis of the linear space $\mathbb{R}^3$, one has,

$$M_{\varepsilon,\varphi}(X) = b + AX + \frac{1}{2}X^T P X e_3,$$

that is,

$$M_{\varepsilon,\varphi}\begin{pmatrix} x \\ y \\ z \end{pmatrix} = \begin{pmatrix} 0 \\ \varphi^2\epsilon \\ \varphi\epsilon \end{pmatrix} + \begin{pmatrix} 1 & \varphi & 0 \\ 0 & 1-\varphi^2 & \varphi \\ 0 & -\varphi & 1 \end{pmatrix} \begin{pmatrix} x \\ y \\ z-\varphi\epsilon x^2 \end{pmatrix}.$$

In particular, we have expressed $M_{\varepsilon,\varphi}$ as the composition of an affine map with a quadratic shear. The result follows from Lemma 5.2 in [24] since, performing the linear change of variables $X = U\xi$, where

$$U = \begin{pmatrix} 0 & \tau & 0 \\ \varphi & 0 & 0 \\ 1 & 1 & 1 \end{pmatrix},$$

where $\tau = Tr(A) = 3 - \varphi^2$, one obtains

$$\tilde{M_{\varepsilon,\varphi}}(\xi) = U^{-1} M_{\varepsilon,\varphi}(U\xi) = U^{-1}b + U^{-1}AU\xi + \frac{1}{2}\xi^T Q\xi e_1, \quad \text{where} \quad Q = -2\epsilon\varphi\tau^2 e_2 e_2^T,$$

that is, the symmetric matrix Q defines the form $Q(\xi_1, \xi_2) = \tau^2 e_2 e_2^T \xi_2^2$. This quadratic form does not verify $Q(\xi_1, \xi_2) = Q(\xi_2, \xi_1)$, which is a necessary condition to have a reversibility R.
As an alternative, one can proceed directly by assuming that exists an smooth reversibility R. Then R verifies $R(p_+) = p_-$ where $p_\pm = (\pm 1, 0, 0)$ are the fixed points of $M_{\varepsilon,\varphi}$. On the other hand, since both $M_{\varepsilon,\varphi}$ and $M_{\varepsilon,\varphi}^{-1}$ are quadratic, R has to linear. From $RM_{\varepsilon,\varphi}R(x) = M_{\varepsilon,\varphi}^{-1}(x)$, one obtains $DM_{\varepsilon,\varphi}^{-1}(p_-) = R(DM_{\varepsilon,\varphi}(R(p_-)) = RDM_{\varepsilon,\varphi}(p_+)$, hence $R = DM_{\varepsilon,\varphi}^{-1}(p_-)(DM_{\varepsilon,\varphi}(p_+))^{-1}$. One has

$$DM_{\varepsilon,\varphi}^{-1}(p_-) = \begin{pmatrix} 1 & -\varphi & \varphi^2 \\ 0 & 1 & -\varphi \\ -2\epsilon\varphi & \varphi + 2\epsilon\varphi^2 & 2 - \varphi^2 - 2\epsilon\varphi^3 \end{pmatrix},$$

and

$$DM_{\varepsilon,\varphi}(p_+) = \begin{pmatrix} 1 & \varphi & 0 \\ -2\epsilon\varphi^2 & 1 - \varphi^2 & \varphi \\ -2\epsilon\varphi & -\varphi & 1 \end{pmatrix}.$$

A direct computation shows that $R = (R_{ij})$ is such that $R_{11} = 1 + 2\epsilon\varphi^3$, which contradicts the fact that $R(p_+) = p_-$.

□

The fact that $M_{\varepsilon,\varphi}$ is not reversible makes the numerical computations more involved. From now on, we will fix $\varphi = 0.1$ for numerical computations.

5.1 Visualizing the dynamics of a three dimensional map in two dimensions

In the case of volume preserving flow, we defined in section 2 a Poincaré section such that the corresponding Poincaré map was an area preserving map. Given a map one cannot define a Poincaré section, but we can do a construction, called slices, that allow us to visualise the dynamics in a system of a dimension reduced by one.
The idea of this method is to consider a hyperplane Σ and plot all the iterates of the map that are at a δ distance of Σ. Note that in this way not all crossing of the orbits are captured, so it can take many iterates to get a suitable number of points in the slice.

In particular, for the Michelson map we have considered the plane $\{z = 0\}$ and compute all the points that are on a slice of width $\delta = 10^{-4}$. In Figure 5.2, a projection of those points to the $\{z = 0\}$ plane is shown. In this case, given an initial condition that do not scape, the maximum number of iterates that we need to obtain 1000 points on the slice is 22332592 for $\varepsilon = 0.14$.

An alternative to this method, is to use an interpolation of the iterates of the map $M_{\varepsilon,\varphi}$. When a crossing x_0 is detected we consider n positive and n negative iterates of the

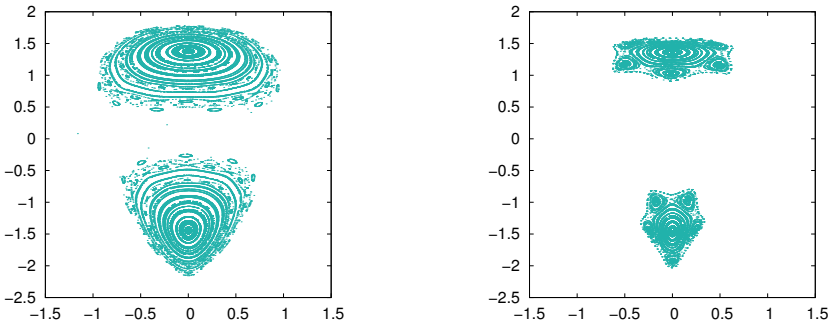

Figure 5.2: Slice of system for $\varepsilon = 0.10$ and 0.14, with a width $\delta = 10^{-4}$.

point and we compute the interpolating polynomial $P_{2n+1}(t)$ of degree $2n+1$ such that $P_{2n+1}(n) = x_n$, where x_n denotes the n-th iterate of the map $M^n_{\varepsilon,\varphi}(x_0)$. Then we plot the intersection of the polynomial with the hyperplane.

Considering the plane $\{z = 0\}$, we plot those intersections for the Michelson system in Figure 5.3, using a polynomial of order 10. Note, that with this method, each time the map crosses the plane we get a point of the plot. The maximum number of iterates of an orbit that do not scape that we need to visualize 1000 point is around 62811 for $\varepsilon = 0.14$.

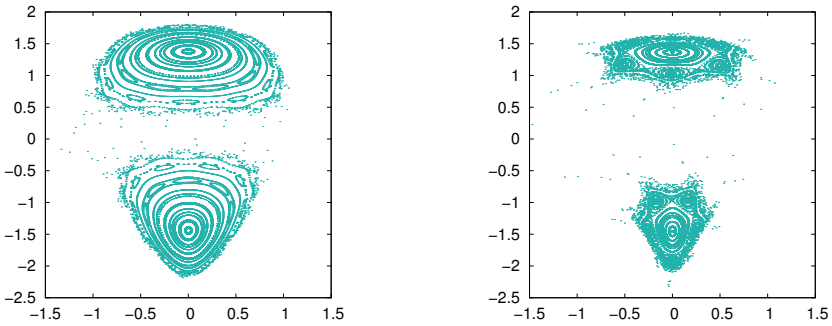

Figure 5.3: Visualization of the intersection of the Michelson map with $\{z = 0\}$ using the interpolation, for $\varepsilon = 0.10$ and $\varepsilon = 0.14$.

The fact that we obtain good visualizations with less iterates helps in analysing the dynamics in higher dimensions as it was stressed in [17]. The derivative of the polynomial at x_0 defines a vector field. For near the identity maps such a vector field can be seen as the vector field obtained by suspension and after performing several averaging steps (depending on the distance to the identity of the map and the degree of the interpolating polynomial) to remove the dependence on time (which is a fast variable of the suspension for close to identity maps, see comments on the suspension and averaging process in section 3.4.1).

Note that the dynamics that we observe using any of the two methods is not two-dimensional,

so we cannot assert the same results as for a volume preserving flow. For example,

- The "fixed point" that we see in the plots corresponds to the intersection of a normally elliptic curve Γ, or of the polynomial that interpolates the iterates of points of the curve, with the plane $\{z = 0\}$. For a fixed value of φ, the rotation number of Γ changes with respect to ε and becomes rational for a dense set of values of ε.

- The curves that we see in the plot are not invariant curves, they are projections of two-dimensional tori of the map. There are KAM theorems adapted to this setting that guarantee the persistence of the tori for the map near Γ, see [13] and [38].

- For an area preserving twist map, the Aubry-Mather theory, see [26, 9], shows that after the destruction of rotational invariant curves, there is a remnant in the phase space, which is a Cantor set (the Aubry-Mather set). There is no analogous of this theory for three dimensional maps. This means that what we do not know the structure of what we observe as invariant curves with holes near the boundary of the stability domain. The mathematical description of the transport properties through the holes remains unknown.

- What seems to be resonant islands in the plots, correspond to three-dimensional resonant structures. It would be interesting to derive a suitable normal form around Γ to analyse and classify such structures, in a similar way as we did for resonant islands of volume preserving flows in section 3.4. Note that since we have three frequencies, there are rank one and rank two resonances, which gives different structures, [14]. A generalization of the Poincaré-Birkhoff theorem 3.8 to this setting, showing the existence of normally hyperbolic invariant curves that maps one into another, can be found in [12].

Concerning the first item of the previous list, we can proceed as follows to illustrate how the rotation number varies with ε. Consider the interpolation procedure explained to get points in $z = 0$. We look for a fixed point x^* on $z = 0$ of the map $G = P \circ M^m_{\varphi,\varepsilon}$ defined as follows. Given an initial point on $z = 0$ we fix m to be the number of iterates that needs the point to complete a revolution near the normally elliptic invariant curve Γ and cross again $z = 0$. The map P maps the final point (after the m iterates) to the corresponding point in $z = 0$ by assigning the intersection of the interpolating polynomial p_n with the plane.

Using jet transport through the Lagrange interpolation algorithm to compute p_n, we can compute DG at the initial point. This allows us to use Newton method to find the fixed point x_* of G. Moreover, if t^* is the value for which $p(t^*) \in \{z = 0\}$ then $\rho = 1/(m + t^*)$ gives an approximation of the rotation number of Γ.

In figure 5.4 we show ρ as a function of ε. For $\varphi = 0.1$ and $\varepsilon < 0.25$ the plot shows that the lowest period expected for points on Γ is 63. If we take values of ε in this range we will observe the iterates of x^* spread along Γ. Taking larger values of φ we can observe rational values of ρ with smaller denominator. For example, for $\varphi = 0.619$ we can determine ε so that $\rho = 1/10$. The iterates of x^* in this case form a periodic orbit of period 10.

In the remaining of this chapter we investigate the existence of heteroclinic connections for the map. Note that the two-dimensional invariant manifolds generically intersect along a one dimensional manifold in a three-dimensional space. This means that we expect to

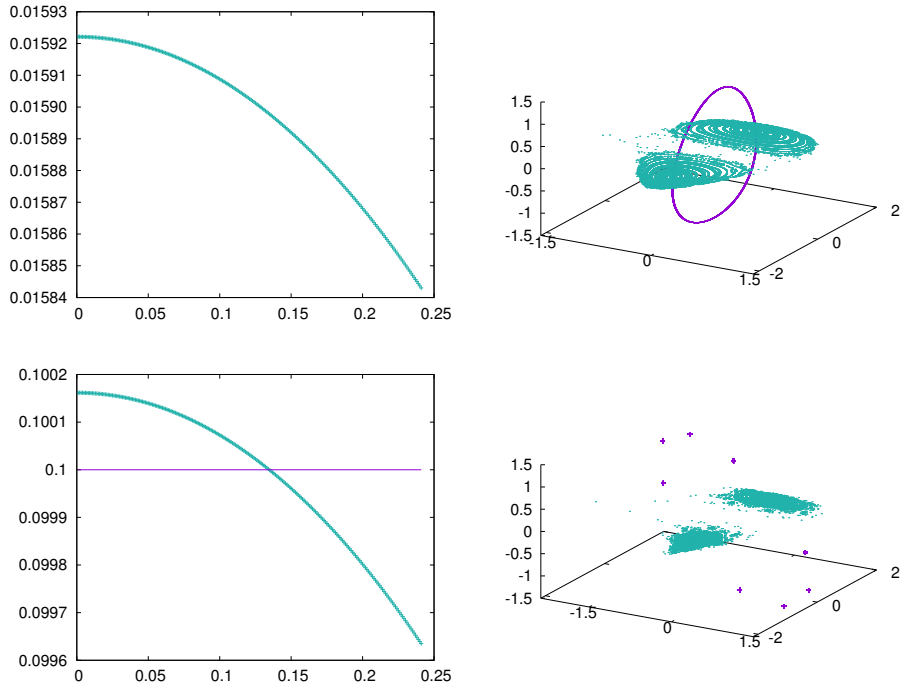

Figure 5.4: Left plots: We display ρ as a function of ε for $\varphi = 0.1$ (top) and $\varphi = 0.619$ (bottom). The green line determines $\varepsilon \approx 0.1347$ for which $\rho = 1/10$. Right plots: We show 1000 iterates of x_* for $\varphi = \varepsilon = 0.1$ (top) and $\varphi = 0.619$, $\varepsilon = 0.1347$ (bottom).

have a continuum of heteroclinic connections, [25]. As far as we know, theoretical results of the splitting of these manifolds are not available, hence a numerical investigation would be of great interest.

5.2 Invariant manifolds and heteroclinic orbits

To compute an approximation of the two-dimensional invariant manifolds of the fixed points $p_\pm$ we use the parametrization method. The idea of the parametrization method is to find a parametrization of $W^u(p_+)$ as a function tangent at p_+ to the two-dimensional eigenspace generated by the eigenvectors of $DF(p_+)$. This leads to the so-called invariance equations.
Let $\Lambda : \mathbb{R}^2 \hookrightarrow \mathbb{C}^2 \longrightarrow \mathbb{C}^2$ be the vector field associated to the eigenvectors of $DF(p_+)$, defined as

$$\begin{pmatrix} s_1 \\ s_2 \end{pmatrix} \longmapsto \begin{pmatrix} s \\ \bar{s} \end{pmatrix} \longmapsto \begin{pmatrix} \mu_{p_+} & 0 \\ 0 & \bar{\mu}_{p_+} \end{pmatrix} \begin{pmatrix} s \\ \bar{s} \end{pmatrix} = \begin{pmatrix} \mu_{p_+} s \\ \bar{\mu}_{p_+} \bar{s} \end{pmatrix},$$

where $s = s_1 + i s_2$.

We consider the parametrization of $W^u(p_+)$, K as a sum of homogeneous polynomials of

degree $r = i + j$, $(u, v, w) = K(s, \bar{s}) = (u(s, \bar{s}), v(s, \bar{s}), z(s, \bar{s}))$, that is

$$\begin{aligned} u = u(s, \bar{s}) &= \sum_{r \geqslant 0} \alpha_{ij} s^i \bar{s}^j, \\ v = v(s, \bar{s}) &= \sum_{r \geqslant 0} \beta ij s^i \bar{s}^j, \\ w = w(s, \bar{s}) &= \sum_{r \geqslant 0} \gamma ij s^i \bar{s}^j. \end{aligned}$$

such that $K(0, 0) = p_+$. Therefore, the invariance equation is given by

$$F(K(s, \bar{s})) = K(\Lambda(s, \bar{s})), \tag{5.2}$$

where $K(s, \bar{s}) = (u(s, \bar{s}), v(s, \bar{s}), z(s, \bar{s}))^T$ and $\Lambda(s, \bar{s}) = (\mu s, \bar{\mu}\bar{s})^T$. This is equivalent to the system

$$\begin{aligned} &\sum_{r \geqslant 0} \alpha_{ij} s^i \bar{s}^j + \varphi \sum_{r \geqslant 0} \beta ij s^i \bar{s}^j - \sum_{r \geqslant 0} \alpha_{ij} \lambda^i s^i \bar{\lambda}^j \bar{s}^j = 0, \\ &\sum_{r \geqslant 0} \beta ij s^i \bar{s}^j + \varphi \left[\sum_{r \geqslant 0} \gamma ij s^i \bar{s}^j + \varphi \left(\varepsilon \left(1 - \left(\sum_{r \geqslant 0} \alpha_{ij} s^i \bar{s}^j \right)^2 \right) - \sum_{r \geqslant 0} \beta ij s^i \bar{s}^j \right) \right] - \sum_{r \geqslant 0} \beta ij \lambda^i s^i \bar{\lambda}^j \bar{s}^j = 0, \\ &\sum_{r \geqslant 0} \gamma ij s^i \bar{s}^j + \varphi \left(\varepsilon \left(1 - \left(\sum_{r \geqslant 0} \alpha_{ij} s^i \bar{s}^j \right)^2 \right) - \sum_{r \geqslant 0} \beta ij s^i \bar{s}^j \right) - \sum_{r \geqslant 0} \gamma ij \lambda^i s^i \bar{\lambda}^j \bar{s}^j. \end{aligned}$$

Solving this system, we will find coefficients α_{ij}, β_{ij} and γ_{ij} that will give us an approximation of the two-dimensional invariant manifold. We will solve the previous non-linear system of equations order by order. At order zero we obtain the condition of being a fixed point of the system. At order one the condition becomes the one of the eigenvectors of DF at the fixed point. Once we choose the desired point $p_\pm$ and normalized eigenvectors associated to $\mu_{p_+}, \bar{\mu}_{p_+}$, the coefficients of order k of the parametrization can be determined since they are solutions of $k + 1$ three-dimensional linear systems with matrices of the form

$$DM_{\varepsilon,\varphi}(p_\pm) - diag(\mu^i_{p_\pm}, \bar{\mu}^j_{p_\pm}),$$

with $i + j = k$, and with right-hand determined by the previous orders. We solve the linear system using, for example, Gaussian elimination with partial pivoting. We use PARI/GP internal routines to facilitate the implementation, [10].

We have done these computations up to order 10. Note that we also need to compute the domain of the Taylor expansion of the invariant manifolds $W^u(p_+)$, where the parametrization gives the desired accuracy (in computations we use 10^{-26} of accuracy with 58 digits in arithmetic computations). Then, inside this domain, we define a fundamental domain that captures an iterate of any orbit on $W^u(p_+)$. Such a domain is an annular region in (s_1, s_2) coordinates, of the form $[rmax/ \mod (\mu_{p_\pm}), rmax) \times S^1$ in terms of polar coordinates in the s_1, s_2 coordinates. We look for an optimal $rmax$ inside the previous domain.

When computing the invariant manifolds of the Michelson flow, we used that the system was reversible, so that computing just one the manifolds we could get the other one directly. In this case there is no reversibility, so we have to compute both two-dimensional

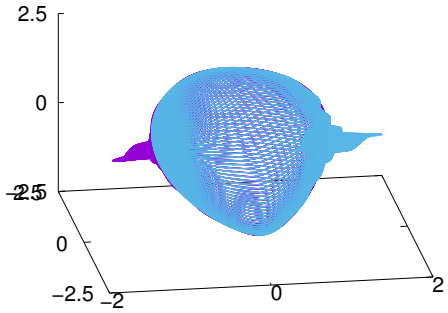

Figure 5.5: Invariant manifolds $W^u(p_+)$ (in purple) and $W^s(p_-)$ (in blue) of the Michelson map, for $\varepsilon = 0.1$ and $\varphi = 0.1$.

invariant manifolds $W^u(p_+)$ and $W^s(p_-)$ using the parametrization method explained above. Once we get the parametrization of both manifolds, we choose points in the fundamental domains that we iterate to get a visualization of the global manifolds. The invariant manifolds for $\varepsilon = \varphi = 0.1$ are shown in Figure 5.5.

We can see that both invariant manifolds do not coincide, and that the two-dimensional invariant manifolds go through the channel created by the one-dimensional manifolds, as we explained in the case of the Michelson flow.
To see this behaviour clearly, we can project a set of orbits on the two-dimensional invariant manifolds onto the plane $\{z = 0\}$ using the interpolation explained in the previous section.

The results are shown in Figure 5.6. In this plot we see that the invariant manifolds does not coincide, and the intersection points correspond to the heteroclinic connections of the map. In this section, we could also study the splitting between the manifolds. However what we see in the plots are projections of orbits of the invariant manifolds onto $\{z = 0\}$ using the interpolation.
As we have mentioned, the Michelson map has heteroclinic orbits lying in the intersection of the two-dimensional stable and unstable manifolds of the two fixed points. The existence of a continuum of heteroclinic orbits for volume preserving maps, was observed in [25].

To compute the heteroclinic orbit, we observed that we have four variables and three conditions. The four variables correspond to (s_1^u, s_2^u) of the parametrization of $W^u(p_+)$ and (s_1^s, s_2^s) of the stable manifold $W^s(p_-)$. The three conditions are the following. We consider suitable number of iterations for points on both fundamental domains, say n_u and n_s respectively. Hence the conditions are

$$M_{\varepsilon,\varphi}^{n_u}(K^u(s_1^u, s_2^s)) = M_{\varepsilon,\varphi}^{n_s}(K^s(s_1^s, s_2^s)).$$

Hence we proceed as follows. We fix a radius r_u on the fundamental domain of $W^u(p_+)$,

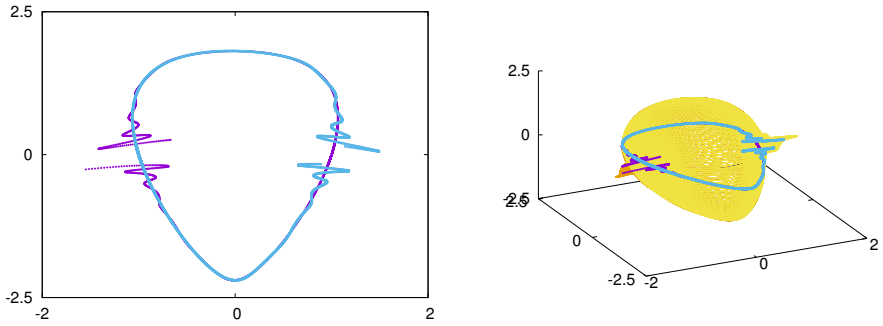

Figure 5.6: Intersection of the invariant manifolds $W^u(p_+)$ and $W^s(p_-)$ with the plane $\{z = 0\}$.

and we define a function

$$Q(r_s, \theta_u, \theta_s) = M^{n_u}_{\varepsilon,\varphi}(\tilde{K}^u(r_u, \theta_u)) - M^{n_s}_{\varepsilon,\varphi}(\tilde{K}^s(r_s, \theta_s)),$$

where (r_u, θ_u), and (r_s, θ_s), are the polar coordinates in the (s^u_1, s^u_2) plane, and (s^s_1, s^s_2) respectively. Thus, we solve the equation $Q(r_s, \theta_u, \theta_s) = 0$ by Newton method.
By changing the fixed radius r_u, we obtain different heteroclinic orbits of the continuum.

For $\varepsilon = 0.1$ and $\varphi = 0.1$ we have computed the parametrization of the stable and unstable manifold up to order 20, requiring a precision of 10^{-26} for points in the fundamental domain. The number of iterations are $n_u = 62$ and $n_s = 445$. The fundamental domain for the unstable manifold is $[rmin, rmax) = [rmax/|\mu_{p_-}|, rmax)$ with $rmax = 0.275$ and $|\mu_{p_-}| \approx 1.019$. In Figure 5.7 we show the heteroclinic orbits computed solving $Q = 0$ with $r_u = rmin$ and $r_u = (rmin + rmax)/2$.

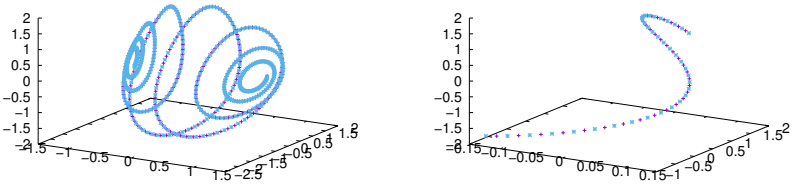

Figure 5.7: An heteroclinic orbit of the Michelson map for $\varepsilon = 0.1$ and $\varphi = 0.1$.

As we already mentioned, we do not know any result describing properly the asymptotic behaviour of the splitting of these manifolds for φ fixed and ε tending to zero. This would be an interesting problem to work on in the near future.

Conclusions

In this work we have studied some properties of conservative three-dimensional flows by using different analytic and numerical techniques from dynamical systems. In particular we illustrated some aspects of the dynamics of the Michelson flow for relatively small values of the parameter.

The reduction of the three-dimensional flow to a Poincaré map leads us to study general results of area preserving maps. We used the Birkhoff normal form around an elliptic fixed point to prove the existence of periodic orbits of the map, along with the structure of resonant islands. We also discussed the persistence of KAM invariant curves when perturbing the system. Last thing we discussed concerning three-dimensional volume-preserving flows, was the behaviour of invariant manifolds and that they have an exponentially small splitting. The phenomena described for the map has been interpreted in terms of the three-dimensional flow, with special emphasis on the Michelson system for which several computations were done.

As pointed out in the introduction, there are many results in the bibliography devoted to conservative three dimensional flows. However, when considering three-dimensional volume-preserving maps, there are still many open questions about their dynamics. Certainly some important results have been generalised to this setting. For example there are versions of KAM theorem's that guarantee the persistence of invariant tori with varying frequency. Also there are generalizations of the Poincaré-Birkhoff theorem. But there are still many other structures in phase space that need further investigations. We devoted the last chapter to emphasize the differences between the continuous and the discrete Michelson systems.

Simple visualizations of the phase space structure showed a resemblance with the flow. Nevertheless, the map is dynamically richer as expected from the fact that it has an extra frequency if we think at the level of its suspension. We showed that the two dimensional tori are organized around a normally elliptic invariant curve. The rotation of such a curve changes with respect to the parameter ϵ of the Michelson system when the parameter φ, which somehow measures the distance to the limit Michelson flow, is fixed to be small and constant. This means that the local dynamics must be analysed in terms of a normal form around such a curve and has to take into account resonances involving the third frequency (the time). Moreover, we illustrated that the Michelson map possesses a continuum of heteroclinic orbits. It remains to investigate the splitting of the 2-dimensional manifolds in the direction transversal to such continuum, which since the map possesses an extra frequency it could be much more involved that the asymptotic behaviour of the splitting for the 3-dimensional flow.

Finally, we would like to mention that most of the theoretical techniques (normal form, suspensions of maps, averaging, exponentially small phenomena, parametrization method) and numerical tools (Taylor ode integrator, jet transport, interpolating polynomials, computation of invariant manifolds) considered during this work can be applied to more general three dimensional or even to analyse the dynamics of higher dimensional systems like, for example, four dimensional maps.

Bibliography

[1] Alessi E. M., Farrès A., Jorba A., Simó C and Vieiro A. *Jet transport and applications to NEOs*, 1st IAA Planetary Defense Conference: Protecting Earth from Asteroids, Granada (Spain), (2009).

[2] Arnold V. *Chapitres Supplémentaires de la Théorie des Equations Diffñerentielles Ordinaires*, Editions Mir. Moscow (1980).

[3] Arnold V. *Mathematical Methods of Classical Mechanics*, Springer-Verlag, (1989).

[4] Arnold V. *Sur la geometrie differentielle des groupes de Lie de dimension infinie et ses applications I. L'hydrodynamique des fluides parfaits*, Ann. Inst Fourier **16**, 316–361. (1966).

[5] Arnold and Khinchin A. Y. *Continued Fractions*, Chicago, IL: The University of Chicago Press, (1964).

[6] Arrowsmith D.K. and Place C.M. *An introduction to Dynamical Systems*, Cambridge University Press (1990).

[7] Batchelor G.K. *An Introduction to fluid dynamics*, Cambridge University Press, (2000).

[8] Baldomá I., Ibáñez S. and Seara T.M. *Hopf-Zero singularities truly unfold chaos*, Commun Nonlinear Sci Numer Simulat, **84**, (2020).

[9] Bangert V. *Mather Sets for Twist Maps and Geodesics on Tori, Dynamics Reported*, Vieweg Teubner Verlag, **1** Wiesbaden, (1988).

[10] Batut, C.; Belabas, K.; Bernardi, D.; Cohen, H.; Olivier, M. *Users' guide to PARI/GP. http://pari.math.u-bordeaux.fr/*.

[11] Broer H.W., Huitema G. B. and Sevryuk M. B. *Quasi-Periodic Motions in Families of Dynamical Systems*, Springer, (1996).

[12] Cheng C. and Sun Y. *Existence of periodically invariant curves in 3-dimensional measure-preserving mappings*, Celestial Mech Dyn Astr **47**, 293-303 (1989).

[13] Cheng C. and Sun Y. *Existence of invariant tori in three-dimensional measure-preserving mappings*, Celestial Mech Dyn Astr **42**, 275–292 (1989).

[14] Dullin H.R. and Meiss J.D. *Resonances and twist in volume-preserving mappings*, SIAM J. Dyn. Sys. **11**, 319-359 (2012).

[15] Dumortier F., Ibáñez S., Kokubu H. and Simó C. *About the unfolding of a Hopf-zero singularity*, Discrete Contin Dyn Syst **33**, 4435-4471, (2013).

[16] Dwivedi S, Herman J., Jeffrey L. C. and van den Hurk T. *Hamiltonian Group Actions and Equivariant Cohomology*, Springer International Publishing.(2019).

[17] Gelfreich v. and Vieiro A. *Interpolating vector fields for near identity maps and averaging*, Nonlinearity **31**, 4263–4289 (2018).

[18] Grote J., Makino K. and Berz M. *High-order Validated Representation of Poincaré Maps*, 324-329, (2005).

[19] Guckenheimer J. *On a codimension two bifurcation, in "Dynamical Systems and Turbulence"* (eds. D. A. Rand and L. A. Young), Lecture Notes in Math., **898**, Springer, Berlin-New York, (1981).

[20] Guckenheimer J. and Holmes P. *Nonlinear Oscillations, Dynamical Systems, and Bifurcations of Vector Fields*, Applied Mathematical Science **42**. Springer-Verlag, Berlin (1983).

[21] Hénon M. *Sur la topologie des lignes de courant dans un cas particulier*, C.R. Acad. Sci. Paris A **262**, 312–314, (1966).

[22] Jorba A. and Zou M. *A software package for the numerical integration of ODEs by means of high-order Taylor methods*, Experimental Mathematics, **14**, 1, 99-117, (2005).

[23] Llibre J. and Zhang X. *On the Hopf-Zero bifurcation of the Michelson system*, Nonlinear Anal. Real World Appl. **12**, 1650-1653, (2011).

[24] H.Lomelí and J.Meiss. *Quadratic Volume preserving maps*. Nonlinearity 11(3), 557-574 (1998).

[25] Lomelí H. E. and Ramírez-Ros R. *Separatrix Splitting in 3D Volume-Preserving Maps*, Siam J. Applied Dynamical Systems **7**, 1527-1557, (2008).

[26] Mather J. N. and Forni G. *Action Minimizing Orbits in Hamiltonian Systems*, Graffi S. (eds) Transition to Chaos in Classical and Quantum Mechanics. Lecture Notes in Mathematics, vol 1589. Springer, Berlin, Heidelberg. (1994).

[27] Meiss J.D., Miguel N, Simó C. and Vieiro A. *Accelerator modes and anomalous diffusion in 3D volume-preserving maps*, Nonlinearity **31**, 5615-5642 (2018).

[28] Meyer K., Hall G. and Offin D. *Introduction to Hamiltonian Dynamical Systems and the N-Body Problem*, Applied Mathematical Science **90**. Springer-Verlag (2009).

[29] Mezic I. *On the geometrical and statistical properties of dynamical systems: Theory and applications*, Dissertation (PhD), California Institute of Technology (1994).

[30] Michelson D. *Steady solutions of the Kuramono-Sivashinsky equation*, Physica D **19**, 89-111 (1986).

[31] Olver P.J. *Applications of Lie Groups to Differential equations*, Springer-Verlag, New York (1986).

[32] Perko. L. *Differential Equations and Dynamical Systems*, 3rd edition. Springer-Verlag. (2001).

[33] RaghavanS. V., McLeod J. B. and Troy W. C. *A singular perturbation problem arising from the Kuramoto-Sivashinsky equation*,Differential Integral Equations, **10**, (1997).

[34] Siegel C.L. and Moser J.K. *Lectures on Celestial Mechanics*, Springer-Verlag, Berlin (1971).

[35] C. Simó. *On the Analytical and Numerical Approximation of Invariant Manifolds*. Les Méthodes Modernes de la Mecánique Céleste (Course given at Goute- las, France, 1989), D. Benest and C. Froeschlé (eds.), pp. 285-329, Editions Frontières, Paris, (1990).

[36] Simó V. and Vieiro A. *Resonant zones, inner and outer splittings in generic and low order resonances of area preserving maps*, Nonlinearity **22**, 1191-1245 (2009).

[37] Sotomayor J. *Lições de equações diferenciais ordinárias*, Rio de Janeiro: IMPA, (1979).

[38] Xia, Z. *Existence of invariant tori in volume-preserving diffeomorphisms*, Ergodic Theory and Dynamical Systems, **12**, 621-631. (1992).